GEOLOGICA CARPATHICA, AUGUST 2022, 73, 4, 273–291 https://doi.org/10.31577/GeolCarp.73.4.1

The Ďumbier–Prašivá high K calc-alkaline granite suite (Low Tatra Mts., Western Carpathians): Insights into their evolution from geochemistry and geochronology

MARIA MARASZEWSKA[1,2,✉], IGOR BROSKA[1], MILAN KOHÚT[1], KEEWOOK YI[3], PATRIK KONEČNÝ[4] and SERGYI KURYLO[5]

[1]Earth Science Institute, Slovak Academy of Sciences, Dúbravská cesta 9, P.O. Box 106, 840 05 Bratislava, Slovakia; geolmara@savba.sk
[2]Department of Mineralogy, Petrology and Economic Geology, Faculty of Natural Sciences, Comenius University, Ilkovičova 6, 842 15 Bratislava, Slovakia
[3]Korea Basic Science Institute, Ochang, 162, Yeongudanji-ro, Republic of Korea
[4]State Geological Institute of Dionýz Štúr, Mlynská dolina 1, 817 04 Bratislava, Slovakia
[5]Earth Science Institute, Slovak Academy of Sciences, Ďumbierska cesta 1, 974 01 Banská Bystrica, Slovakia

(Manuscript received March 4, 2022; accepted in revised form June 16, 2022; Associate Editor: Katarína Bónová)

Abstract: The geochemistry of major Low Tatra granitic types, namely Prašivá porphyritic Bt (biotite)-granodiorite and Ďumbier Bt-tonalite, indicate their derivation from initial hybrid magmas and represent a mixture among several magma pulses formed via melting of the heterogeneous lower crust. The high K calc-alkaline peraluminous character, along with high Ba, Sr + LREE contents correspond to the partial melting of K-rich mafic and the intermediate hydrated lower crustal source in equilibrium with amphibole or possibly garnet with variable involvement of metasedimentary and/or felsic metaigneous sources. The zircon isotopic age of 360.4±2.7 Ma recorded from diatexite reflects the timing of high-temperature metamorphism of subducted continental crust, and thus corresponds in an initial anatectic process within the present Tatric Unit. The magmatic ages are in the largely overlapping sequence of 353±2 Ma for the Ďumbier tonalite and 352±3 Ma and 351.9±2.9 Ma for Prašivá *Aln (allanite bearing)-subtype* and *Mnz (monazite bearing)-subtypes*, which indicate successive multiple emplacement of magma batches and natural evolution towards their more crustal character. Magmatism in the Low Tatra Mts. represents a post-collisional plutonic system related to the slab break-off mechanism described in the close Malá Fatra crystalline basement as well. Heat from mantle upwelling and volatiles from previous subduction forced the melting of the lower crust towards K-rich mafic or intermediate lithologies, as well as during the emplacement of long-lasting melting of felsic metasedimentary crustal sources. The crystalline core of the Low Tatra Mts. is another example of composite granite pluton in the Western Carpathians, which represents a product of the multiphase Late-Variscan post-collisional setting.

Keywords: Western Carpathians, granitic rocks, Nízke Tatry crystalline basement, petrology, SHRIMP dating, zircon, monazite

Introduction

The Variscan crystalline basement in Europe is exposed in a belt that extends from the Iberian Massif to the Bohemian Massif and later continues in a dismembered course beyond the Alpine front to various Variscan segments. In brief, its formation encompasses late Cadomian rifting, followed by dual subduction of the Rheic and Paleo-Tethys oceans, as well as the final collision of the Gondwana and Laurussia plates along with an involved system of several minor basins and terranes (e.g., Matte 1986; Kroner & Romer 2013; Schulmann et al. 2014). The subduction–collision–extension sequence was connected with long-lasting partial melting of different crustal and mantle sources, which resulted in widespread plutonism for each section of the current Variscan belt (Finger et al. 1997). The post-collisional magmatism characterises composite plutons formed mostly from crustal sources or with a CPG and MPG character (Cordierite and Muscovite Peraluminous Granites, using Barbarin classification) (Barbarin 1990, 1999). Coeval intrusion of high-K Calc-alkaline metaluminous to peraluminous Granites (KCG), which represent hybrids of mantle and crustal related magmas and K–Mg mafic to intermediate magmas, were derived from an enriched mantle source (Moyen et al. 2017; Bonin et al. 2020).

The pre-Alpine crystalline basement of the Western Carpathians is composed of medium- to high-grade metamorphic complexes and intrusives of felsic magmas (e.g., Petrík & Kohút 1997; Broska & Uher 2001), which are exposed within the Cretaceous stacked nappes forming the Tatric, Veporic, and Gemeric Units (Plašienka et al. 1997). The Variscan granitoid rock used to be traditionally subdivided into S-type orthogneisses, which are granites with affinity to both S-type (or CPG to MPG like) and I-type (KCG to ACG – Arc Calc-alkaline Granites). This division is based on the generally-accepted classification of Chappell & White (1974), as well as monazite–allanite distribution in granites (Petrík & Broska 1994), zircon typology (Broska & Uher 1991), biotite composition (Petrík 1982), and Rb–Sr data (Kráľ 1994).

The Devonian/Missisippian magmatism was followed by Permian A-type (KCG) granites and Gemeric rare-metal granites (Petrík et al. 1994; Petrík & Kohút 1997; Broska & Uher 2001; Ondrejka et al. 2021; Villaseñor et al. 2021).

The majority of granitoid suites, which had been classified as either S- or I-types, are the products of a different oxidation regime that had been determined from biotite composition: the I-type shows a primary water content up to 5 wt. % and S-type only 2–4 wt. % (Broska et al. 1997). The hybrid character of both I- and S-type granites was proven by magma mixing from various sources (Kohút & Nabelek 2008; Magna et al. 2010; Broska et al. 2013). The timing of Meso-Variscan magmatism is also disputable; mainly whether the I-type granitoids were followed by the S-type granites (Broska et al. 2013) or were nearly coeval (Kohút & Larionov 2021). Studies in the last two decades, as well as the application of SHRIMP dating and isotope fingerprinting techniques have specified the time frame of magmatic episodes in Variscan times. The aim of this contribution is to present new geochemical and geochronological data on granite evolution in the Tatric part of the Low Tatra Mts., thereby shedding new light for a better understanding of the late-Variscan granite magmatism within the Tatric basement of the present-day Western Carpathians.

Geological setting

The Low Tatra pluton (LTP) is an exposure of the Tatric crystalline basement within the Western Carpathians that encompasses a high-grade metamorphic segment and granitoid pluton formed by several granite types. The pre-Alpine crystalline basement in the Tatric Unit is subdivided into the older, high-grade Lower Étage and the younger, low-grade Upper Étage (Kohút 2020). The Lower Étage is of Cambrian to Silurian in age and composed of a layered amphibolite complex (LAC) with remnants of retrogressed eclogites (Janák et al. 2009), as well as meta-ultramafites, tonalitic gneisses, and sheared Cambrian–Ordovician orthogneisses (Korikovsky et al. 1998; Janák et al. 2020). These meta-igneous rocks are intercalated with metamorphosed psammites/pelites (paragneisses) with rare carbonate (calc-silicate) lenses and scarce black schists. The Upper Étage is formed by Upper Silurian–Devonian volcano-sedimentary sequences composed of metagreywackes, phyllites, metabasites (epidote–actinolite amphibolites). In the Low Tatra Mts., orthogneisses occur in a wide range of textural varieties from banded to augen, and correspond compositionally to a peraluminous, silica-rich, two-mica granite precursor (Petrík & Konečný 2009). In the western part, the tectonic boundary between the granitoid complex and orthogneisses is marked by a zone of migmatites that also occur as tectonic blocks within granitoids. The LAC is composed of different varieties of amphibolites, leptynites, and metatonalites (Hovorka & Méres 1997). The igneous precursors of orthogneisses and metabasic sequences formed during the Cambrian–Ordovician rifting of the Gondwana margin in a back-arc setting (Putiš et al. 2008, 2009).

A characteristic feature of the LTP is textural, petrographic, and chemical variability, which was recognised and classified by Koutek (1931) by several types (Fig. 1b). The NW part of the LTP consists of porphyritic Prašivá Bt(biotite)-granite–granodiorite, while the NE part is formed by Ďumbier Bt(biotite)-tonalite–granodiorite. The Prašivá granitoid contains numerous enclaves (up to tens of centimetres in diameter) of

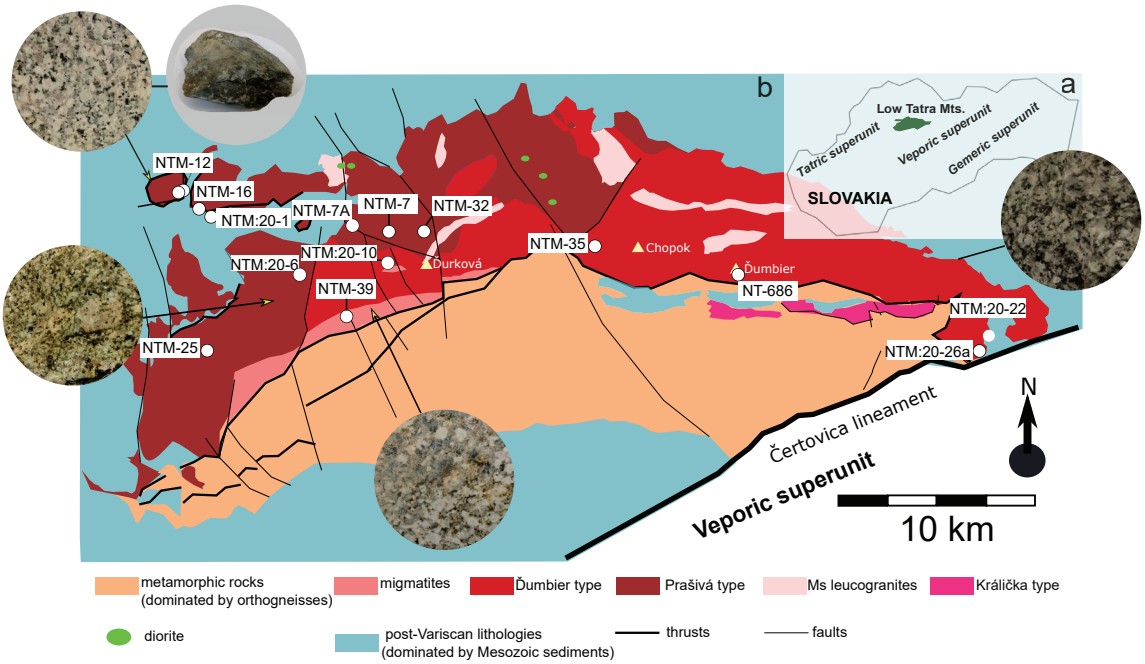

Fig. 1. Simplified geological map of Tatric part of the Low Tatra Mts. (modified after Biely et al. 1992) with sample locations and textures of principal granite types. Inset top right showing location of the Low Tatra Mts.

Bt- or Amp (amphibole)–Bt quartz diorite, which are especially abundant in the SW part in the area of Liptovská Lúžna (Broska & Petrík 1993; Poller et al. 2005). Larger bodies (up to tens of metres) of dioritic rocks also occur in the areas of the Bor peak and the Malé Železné Valley (Spišiak et al. 2017). Muscovite- or two-mica leucogranites form small, elongated bodies (from a few to several hundreds of metres) within the Ďumbier and Prašivá types exceptionally (e.g., in the Dúbrava mining district, the area of Chabenec, or Demänovská Dolina) within the low-grade phyllites from Malé Železné in the Klinisko Valley. Leucogranite bodies show an orientation parallel to the tectonic boundary between the metamorphic complex and the Low Tatra granite intrusions, as well as a system of NNE–SSW faults. The migmatized orthogneisses were intruded by bodies of muscovite–biotite granite assigned to the Ordovician Králička granite type (Dupej & Siegl 1984; Petrík 2000). In the area of Chopok, the xenotime-rich granitoid (Chopok type after Petrík 2000) is interpreted by Burda et al. (2020) as Ordovician "cold granite", which likely represents a roof pendant captured by the late-Variscan Ďumbier granitoid intrusion (Kohút & Larionov 2021). The area of the Low Tatra Mts. is particularly rich in diversified, polymetallic ore mineralization (see Chovan et al. 1996 for review), including Variscan metamorphogenic / magmatic high temperature W–Mo–Au±Sb mineralisation, followed by hydrothermal Sb, Pb–Zn, Pb (Majzlan et al. 2020a,b).

Methods

The investigated rock samples represent over 60 samples of different granitoid types collected across the LTP (Fig. 1b and Supplementary material 1 – SM1). The polished, thin sections of the rocks were used for petrographic and mineralogical research, including modal granite compositions. A set of 5–10 kg weight samples without significant features of weathering, were crushed, grinded, and pulverized. Whole-rock analyses were performed at the Bureau Veritas by ICP-MS lithium borate fusion. The basic geochemical assessment of the analyses was performed using GCDkit free software (Janoušek et al. 2016).

Four representative granitic samples were sent for sensitive high-resolution ion-probe SHRIMP IIe/MC U–Pb isotope measurement to the Korea Basic Science Institute (KBSI) in Ochang (Fig. 1; NTM-39, NTM-12, NTM:20-22 and NTM-32). Zircon grains were separated from crushed, sieved, whole-rock powder using hydraulic, magnetic, and heavy liquid techniques, and were handpicked under a binocular microscope. Selected grains were mounted in epoxy with FC1 (Duluth gabbroic anorthosite, 1099 Ma; Paces &Miller 1993) and SL13 (Sri Lankan gem zircon; U = 238 ppm; Roddick & van Breemen 1994) reference zircons, and ground to expose internal zones. Before analysis, the grains were photographed with an optical microscope, and their internal zoning was imaged by cathodoluminescence (CL) and back scattered electron (BSE) using a JEOL 6610LV scanning electron microscope (SEM) at the KBSI. Procedures of SHRIMP analysis are similar to the protocols described by Williams (1998). A 6–8 nA mass filtered O_2^- primary beam was focused on a spot of approximately 25 μm in diameter on the polished surface of a target zircon grain. Each spot was rastered with the primary beam for about 2 minutes prior to analysis, and then analysed for five cycles with a single electron multiplier. During one cycle, the magnet was stepped through nine peaks of $^{90}Zr_2{}^{16}O$ (counting time = 2 s), ^{204}Pb (10 s), ^{206}Pb (10 s), ^{207}Pb (20 s), ^{208}Pb (5 s), ^{238}U (5 s), $^{232}Th^{16}O$ (2 s) and $^{238}U^{16}O$ (2 s) and 204.1 (10 s; background position). Data processing was conducted using SQUID 2.50 (Ludwig 2009), and the concordia plots were produced using Isoplot 3.75 (Ludwig 2012) programs. Weighted mean ages of zircon were calculated using ^{207}Pb-corrected $^{206}Pb/^{238}U$ ratios after excluding outliers under a statistical t-test and reported at 95 % confidence. Common Pb was removed following the ^{207}Pb (for dates <1000 Ma) correction method using the model by Stacey & Kramers (1975). The entire dataset of zircon dating results is included in SM2.

Monazite age was carried out by the electron microprobe, CAMECA SX 100, which is housed in the State Geological Institute of Dionýz Štúr in Bratislava (Slovak Republic). The main principles of dating procedure were published by Konečný et al. (2018); however, succeeding improvements that were recently added have not been published yet. The measuring conditions (15 kV accelerating voltage and 180 nA beam current, 3 μm beam current) remained the same. A complete analysis was acquired, including REE's, As, Sr, S, Si. Long counting times for elements critical to dating were implemented; for example, 300 s on PbMα (LPET), 80 s on UMβ, 35 s on ThMα, and the same time in the background. Cerrusite, uraninite, and thorianite were used for calibration of Pb, U, and Th. The non-linear background height at PbMα position due to distant background points was estimated using an original method described in this paper (function of curvature to mean atomic number). Numerous peak interferences were corrected via ZAF implemented empirical procedure. The most important were PbMα overlapped by ThMζ1, ThMζ2 and YLγ2,3, UMβ overlapped by multiple ThMζ, ThM3-N4 and ThM5-P3 lines and other interferences among REE's listed in this paper. Detailed examination revealed interference of combined UMζ1 and UMζ2 peaks whose distant tail interfered with the PbMα background point at a relative position of −3255 sinθ*10-5 (CAMECA R = 160 Rowland circle) from the peak position. The other interference at the same background point comes from weak self-interference of PbM4-O2. Both interferences compromising background at PbMα (−3255 sinθ*10-5) were carefully measured and removed. To prove that the microprobe is capable of producing reliable ages, a procedure called MARC (monazite age reference calibration) may indicate and suppress any unwanted systematic errors that may degrade the dating accuracy regardless of the number of analyses accumulated. Fine tuning by calibration lines derived from measurements on monazites (ΔPb vs. Th and ΔPb vs. Y where ΔPb is deviation from the

reference age) with well-constrained ages by SIMS, TIMS, SHRIMP, improves the reliability of dating. Calibration lines are constructed by using 5 age monazite reference materials (ARM's). With an increasing number of reference monazites, the confidence in age estimation grows, while the lines are better constrained. Using high beam currents causes "beam damage" at the analysis spot and is the reason for beam current instability. A time-dependent correction procedure was applied to re-adjust the correct counting ratios between Th–U–Pb and Y (the last was because of interference with PbMα). The spot dating results were evaluated using Isoplot 3.75 (Ludwig 2012). The entire dataset of monazite dating is included in SM3.

Results

Petrographic and geochemical characteristics

Migmatite zone

The representative diatexite from the Jasenie–Kyslá area (NTM-39) is a nebulitic and coarse-grained granodiorite with weak foliation and lineation (Fig. 2a). The rock forming mineral components represent plagioclase ($An_{28–22}$), highly aluminous K-feldspar (Al_{tot} = 1.63–1.65), and moderately ferrous biotite (Fe# ~0.51) intergrown with phengitic muscovite and quartz. Both K-feldspar and quartz show cuspate boundaries and penetrative contact with plagioclase (Fig. 2c), thus indicating disequilibrium that the rock was partially molten (Sawyer 1999). Accessory minerals include abundant monazite-(Ce) (as inclusions in biotite either in feldspars), zircon, and rutile.

Stromatitic migmatite from the Skalka locality shows a granite composition, pronounced discontinuous foliation, well-defined segregation into biotite-dominated, and feldspar/quartz dominated "layers" (Fig. 2b). The composition of plagioclase, K-feldspar, and micas is similar to diatexite; however, it shows a more felsic composition and also contains fibrolite sillimanite intergrown with biotite and muscovite, as well as graphite lenses in mica, possibly implying derivation from paragneisses.

Diatexite from the anatectic zone, as well as migmatites in the SE part (data from Dupej & Siegl 1984) vary on the R1–R2 diagram between granodiorite and granite (Fig. 3a), they are magnesian and highly peraluminous (Fig. 3b). Diatexite is calc-alkaline (Fig. 3c) and shows K_2O/Na_2O equal to 0.5, whereas migmatites are high-K with K_2O/Na_2O, varying 1.15–2. Diatexite is characterised by a high abundance of REE and enrichment in LREE and MREE, as well as a pronounced Eu negative anomaly (Fig. 3d). Diatexite shows a moderate Sr/Y ratio ca. 19; however, a high La/Yb (36) (Fig. 3f and g). The elevated Zr, Th, and U content in diatexite determines the high zircon and monazite saturation temperatures (784 and 830 °C, respectively; Fig. 4a; SM1). The source discrimination diagrams of Patiño Douce (1999) and Sylvester (1998) show that both of the orthogneiss complexes, diatexite and migmatites, are derived from a metaigneous source (Fig. 4b, c, d); however, in Fig. 4e (Laurent et al. 2014), these migmatites fall in the field of a metasedimentary source.

Ďumbier type

The Ďumbier granitic type varies from tonalite to granodiorite and is distinguishable from the Prašivá type due to its darker colour and equigranular structure (Fig. 1). It is composed of euhedral plagioclase and biotite with intergranular quartz and rare K-feldspar. The central parts of the intrusion have a massive structure, as well as grading to a foliated character in marginal parts, which is defined by a subparallel orientation of plagioclase and micas (Siegl 1970; Fig. 2d). Plagioclase often creates a blocky, mosaic microfabric (Fig. 2e) and shows magmatic zonation, while the anorthite content extends from $An_{36–30}$ in the core to $An_{29–25}$ in the rim (Fig. 2f; Maraszewska et al. 2019a). K-feldspar ($Ab_{4–7}$, BaO <1.5 wt.%; Maraszewska et al. 2019b) is subordinated and occurs as near interstitial monocrystalline accumulations (Fig. 2f) with exceptionally larger porphyritic phenocrysts reminiscent of the former definition of the Prašivá type (see below). Lath-shaped biotite is abundant (up to 20 vol.%) and occurs as aggregates as well as streaks flowing around the plagioclase; it is predominantly phlogopite in composition (Al_{tot} = 1.46–1.55 and Mg# = 0.45–0.53; Maraszewska et al. 2019b). Quartz together with K-feldspar form an intergranular phase as irregular grains that are brittle and deformed locally, as well as recrystallized. Accessory minerals are mainly abundant by zircon and apatite inclusions in biotite along with altered grains of allanite. Monazite-(Ce) and xenotime-(Y) are mostly hosted by K-feldspar or quartz rather than by biotite.

The Ďumbier type plot on the R1–R2 diagram shows a composition of tonalite to granodiorite (Fig. 3a). It has a magnesian character using terminology by Frost et al. (2001) and is low to moderate peraluminous (ASI = 1.1–1.19) and relatively high FeO_{tot}, MgO, and TiO_2 (SM1; Fig. 3b). Maficity tends to weakly decrease with aluminosity, similar to the trend of KCG (Fig. 3b). The Ďumbier type belongs to the high-K calc alkaline series (Fig. 3c) with variable K and Na relation (K_2O/Na_2O = 0.6–1.2). Ďumbier granitoids have very high total REEs contents with fractionated REE chondrite-normalised patterns (Fig. 3d) and Dy/Yb 2.0–3.36. The Ďumbier type is Sr and Ba-rich (up to 650 and 1300 ppm, respectively; SM1) and shows the lowest Rb/Ba and Rb/Sr ratios among all the investigated types and corresponds to the field of high Ba–Sr granitoids, which means "adakites" feature (Fig. 3e). Adakitic s.l., or "TTG" (trondhjemite–tonalite–granite)-like signature reflects the high ratios of Sr/Y (38–55) and La/Yb (26–58; Fig. 3f, g) as well. The high Zr and REE bulk rock contents lead to high zircon saturation temperature (744–808 °C; Boehnke et al. 2013; Fig. 4a), as well as Mnz saturation temperatures (750–820 °C; Montel 1993); however, they are lower than experimental melts with similar FeO and MgO content derived from the dehydratation melting of mafic sources,

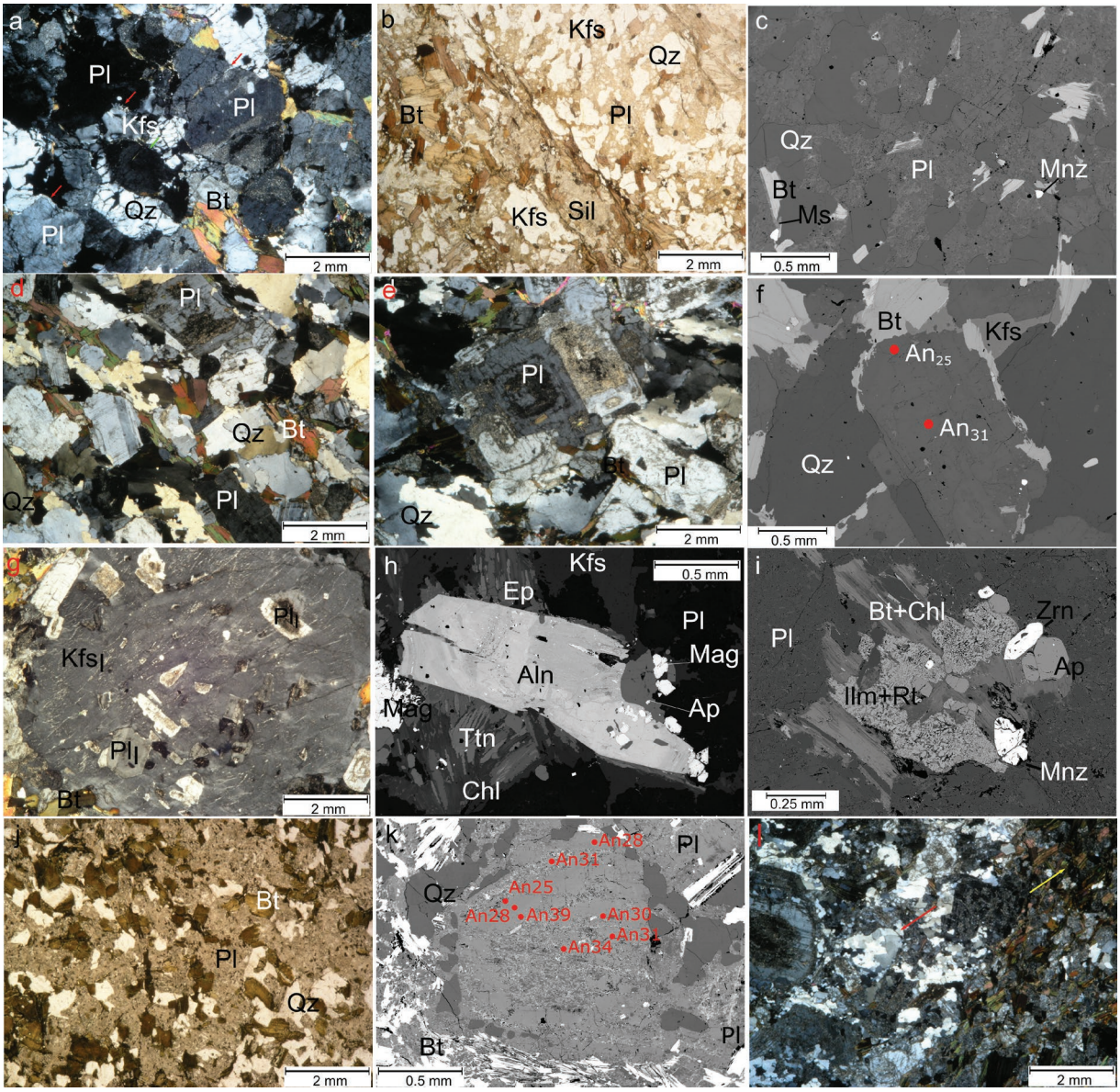

Fig. 2. Microfabrics and petrography of investigated granitoids: **a** — Coarse grained diatexite (NTM-39) – quartz and K-feldspar show cuspate contact with plagioclase (red arrow) indicating reaction of plagioclase with melt; **b** — Foliated stromatitic sillimanite-bearing migmatite; **c** — Microfabric of Sil-bearing migmatite; note the strongly embayed boundaries of plagioclase crystals with cuspate quartz grains (BSE); **d** — Cumulate-like texture of Ďumbier tonalite; **e** — Euhedral, normal zoned plagioclase grain in the Ďumbier type; **f** — Normal magmatic zonation of plagioclase in the Ďumbier type; **g** — K-feldspar porphyrocryst in the Prašivá Mnz-subtype; **h** — Accessory, altered allanite-Ce, magnetite and apatite rimmed by secondary titanite and epidote in Aln-subtype of Prašivá (BSE); **i** — Accessory monazite, apatite, zircon and ilmenite hosted by biotite aggregates in mnz-Prašivá (BSE); **j** — Bt-rich fine-grained enclave; **k** — Subhedral oscillatory-zoned plagioclase phenocryst in enclave; note the sponge-like outermost rim filled up by quartz inclusions; **l** — Contact zone between Prašivá granite and MME (yellow arrow); note the characteristic hybridisation textures formed by altered plagioclase phenocrysts which rimm quartz and quartz ocellis (red arrow). Abbreviations here and herein: Qz=quartz; Pl=plagioclase, Kfs=K-feldspar, Ms=muscovite, Bt=biotite, Aln=allanite, Mnz=monazite, Ap=apatite, Zrn=zircon, Rt=rutile, Ilm=ilmenite, Ttn=titanite, Chl=chlorite, Ep=epidote, Mt=magnetite, Sil=sillimanite.

which may indicate water-present melting. The Ďumbier granitoid compositions are consistent with the basalt-derived experimental melt with mutual transition to the metagreywacke melt in the plots of Patiño Douce (1999) (see Fig. 4b, c), whereas mafic K-rich source is reflected in the discrimination diagram by Laurent et al. (2014; Fig. 4e).

Prašivá type

The Prašivá granite type represents a medium- to coarse-grained biotite-granodiorite to granite, with K-feldspar megacrysts extending up to 2–3 cm in diameter (Figs. 1b, 2g) – the porphyritic fabric is especially pronounced in the south

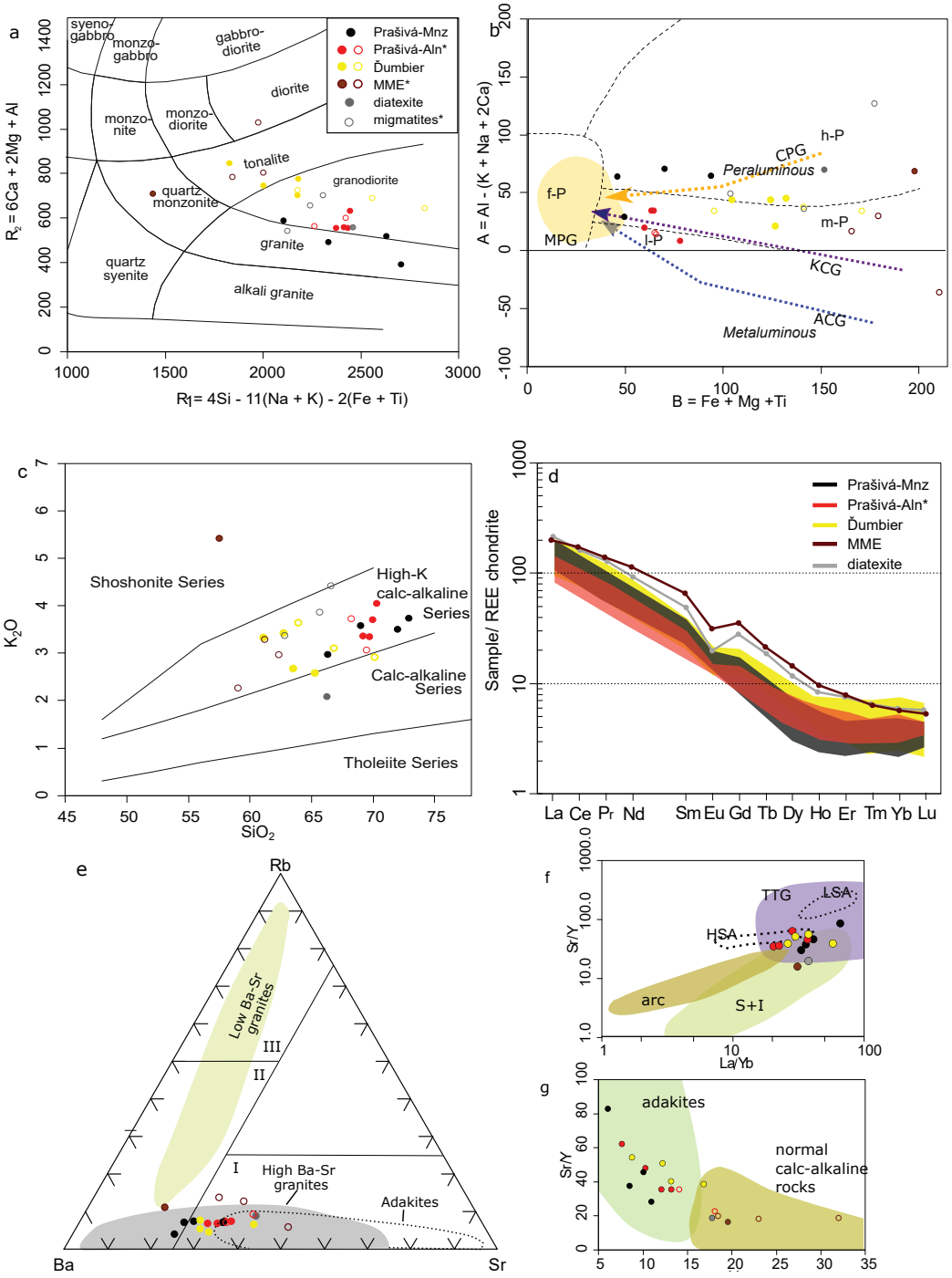

Fig. 3. Major and trace element geochemistry of granitoids in the Low Tatra Mts: **a** — Projection on R1–R2 plot (after De la Roche et al. 1980) – Ďumbier type plots on tonalite-granodiorite fields, whereas Prašivá Aln-subtype is granodiorite and the Mnz-subtype shows transition from granodiorite to granite. Enclaves hosted by the Prašivá Aln-subtype, which represents tonalite to diorite, whereas the enclave hosted by Prašivá Mnz-subtype is quartz monzonite; **b** — B–A diagram by Villaseca et al. (1998) with trends of Barbarin's (1990, 1999) granitoid types after Bonin et al. (2020) and Jacob et al. (2021) – note the higher maficity of the Ďumbier type than the Prašivá types. The Ďumbier and Prašivá Aln-subtypes show a trend similar to KCG, whereas the Mnz-subtype shows parameters evolving towards CPG; **c** — Peccerillo and Taylor (1976) discrimination of normal-, medium-, high- and ultra-high K rocks emphasising overall high-K character of LTP granitoids; **d** — Chondrite-normalised REE diagram (Boynton 1984) of granites: note the high fractionation of LREE/HREE in all investigated granitoid types; **e** — Rb, Ba and Sr relations in the Low Tatra's granite field (Tarney & Jones 1994, modified): I (low evolved), II (midly evolved), and III (high evolved) correspond to the typology of Western Carpathian granites according to Broska & Uher (2001); **f** — Sr/Y vs La/Yb diagram (after Moyen 2009) discriminating TTG (trondhjemite–tonalite–granodiorite suites), HSA (High Silica Adakites), LSA (Low Silica Adakites), normal S- and I-type granitoids and arc magmas – note that the Ďumbier and Prašivá granitoids plot in the TTG or HSA field; **g** — Sr/Y vs Y diagram distinguishing adakitic magmas and normal arc magmas (adapted from Defant & Drummond 1990). Explanations: Full symbols = new data; open symbols = migmatite data from Dupej & Siegl (1984); enclaves data from Poller et al. (2005).

part of the massif. The Prašivá granitic suite manifests compositional heterogeneity emphasised by an accessory mineral assemblage leading to subdivision into the *Aln-bearing subtype* in the NW part (Fig. 2h; Maraszewska et al. 2019a), and the *Mnz-bearing subtype* (Fig. 2i) in the central and southern part of the LTP. The Prašivá granitoid hosts up to tens of centimetres in diameter, spherical, Amp- or Bt-diorite microgranular enclaves (Fig. 2j), which are especially abundant within *Aln-subtype* in the NW part of the LTP near the village of Liptovská Lužná. The enclaves themselves (including the interface between them) and host Prašivá granites can be marked as microtextural indicators of mixing and mingling (Hibbard 1981; Baxter & Feely 2002) along with oscillatory zoning of plagioclase megacrysts (Fig. 2k), rounded quartz ocelli's, biotite clots (Fig. 2l), and acicular apatite.

Except for biotite, the composition of rock-forming minerals is similar across the pluton. K-feldspar forms oval or lath-shaped porphyrocrysts, as well as smaller, anhedral, interstitial grains. The porphyrocrysts show oscillatory or reversed concentric zonation in BaO (up to 2 wt.%) correlated with X_{Ab} (up to 10 mol.%; Maraszewska et al. 2019a). Growth zones are marked by the presence of oriented biotite and plagioclase inclusions (Fig. 2g), whereas interstitial grains are usually Ba-poor. Euhedral plagioclase contains $An_{35–32}$ in patchy central zones, while the rims are usually oligoclase–albite in composition. Biotite usually forms aggregates and varies between phlogopite (*Aln-subtype*) and annite (*Mnz-subtype)*; if muscovite is present, it is only secondary (Maraszewska et al. 2019a, b) Quartz occurs as recrystallized aggregates in the matrix; in the *Mnz-subtype*, also as a cuspate in K-feldspar, where it usually shows sutured, lobate grain boundaries. In the *Aln-subtype*, accessory mineral assemblage includes REE zoned apatite, zircon, hematite, orthomagmatic Al-poor and REE-rich allanite (Fig. 2h; Maraszewska et al. 2019a), while in the *Mnz-subtype*, apatite, zircon, ilmenite, hematite, and monazite-(Ce) dominate (Fig. 2i).

Aln-subtype corresponds to granodiorite on the R1–R2 diagram (Fig. 3a). It is weakly to moderate peraluminous (Fig. 3b) and slightly higher in CaO composition (SM1) than the *Mnz-subtype* granite–granodiorite (Fig. 3a), which is peraluminous to highly peraluminous (Villaseca et al. 1998; Fig. 3b). Both the *Mnz-* and *Aln-bearing* Prašivá subtypes belong to the high-K calc-alkaline series (Fig. 3c) and show a magnesian character like the Ďumbier type (Frost et al. 2001; SM1). Uniformily, both subtypes show trends between KCG and CPG and increase in LILE with respect to HFSE. However, *Aln-subtype* as metaluminous to subaluminous granite reflects a KCG character, whereas the *Mnz-subtype* is closer to CPG by higher aluminosity. Both subtypes show similar trace element compositions: a high ΣREE content with steep, HREE-depleted patterns and variable Eu* (Fig. 3d); however, in contrast to the Ďumbier granite type, the *Aln-subtype* shows a slightly more convex upward pattern in MREE. The Prašivá type generally shows distinctively lower Dy/Yb ratios (1.8–2.4). Moreover, the Prašivá type shows high Sr/Y (35–85) and La/Yb (21–66) ratios like high-silica adakites, TTG on Moyen's discrimination diagrams (2009), or adakites on Defant & Drummond's (1990) discrimination diagrams (Fig. 3f, g). Prašivá subtypes plot in the field of high Ba–Sr granites (Ba = 700–1540 ppm, and Sr = 300–500 ppm; Fig. 3e) with Rb/Ba ratio ~0.11 and Rb/Sr 0.22–0.30 (SM1). *Mnz-subtype* shows a surprisingly slightly elevated zircon saturation temperature (706–796 ºC Boehnke et al. 2013) as well as monazite saturation temperatures (800–830 ºC; Montel 1993) in comparison to *Aln-subtype* (702–725 and 740–800 °C, respectively; Fig. 4a; SM1). Overall, the Prašivá granitic type reflects a hybrid character and evolution from basalt-derived melt for the *Aln-subtype* to metagreywacke-derived melt for the *Mnz-subtype* (Fig. 4b, c, d) or high-K mafic to metatonalitic, respectively (Fig. 4e).

Mafic microgranular enclaves in the Prašivá type

Mafic enclaves hosted by the *Aln-Prašivá subtype* in the Ráztočná Valley vary from diorite to tonalite (Fig. 3a); they are subaluminous to metaluminous with higher Ca, Mg, Fe + Ti than host granitoids (Fig. 3b). Enclaves emplaced within the *Mnz-subtype* in the SW part of the intrusion show much higher aluminosity and lower Ca content. Nevertheless, all analysed enclaves plot to a high-K calc-alkaline field (Fig. 3c) and are characterised by a very high REE content (up to 230 ppm in total), as well as fractionated REE patterns (Fig. 3d) and decreasing Sr and Ba contents with respect to Rb (Fig. 3e). They also show low Sr/Y ratio (<20) projection to the field of normal arc magmatic rocks (Fig. 3f, g). Due to equilibration, zircons and monazite saturation temperatures of the enclaves are comparable to the host granites (Fig. 4a; SM1). In essence, enclaves show a composition of magmas from basaltic/metasedimentary mixed sources (Fig. 4b, c, d). However, the source discrimination diagram of Laurent et al. (2014) (Fig. 4e) indicates that the enclaves hosted by the *Aln-subtype* are consistent with a K-rich mafic source, whereas enclaves hosted by the *Mnz-subtype* are consistent with metasedimentary sources. Compositional variability of the enclaves seems to depend on the degree of their re-equilibration with granitic magmas.

Zircon SHRIMP U–Th–Pb dating

Zircon morphology

Cathodoluminescence (CL) zircon growth images show variable habit and zonation patterns (Fig. 5). Diatexite zircons show a wide range of morphological types, but the most characteristic zircons are large, up to 400 µm, strongly-elongated with irregular or convolute discontinuous sector zonation, sometimes homogenous crystals with rounded edges (grains NTM-39_9 or NTM-39_2 on Fig. 5). There are also prismatic crystals with typical concentric magmatic and concentric multiple zonation (grain NTM-39_5 or NTM-39_12). In the Ďumbier and Prašivá granitic types, zircon grains vary in size 100–500 µm and show relatively high elongation. These

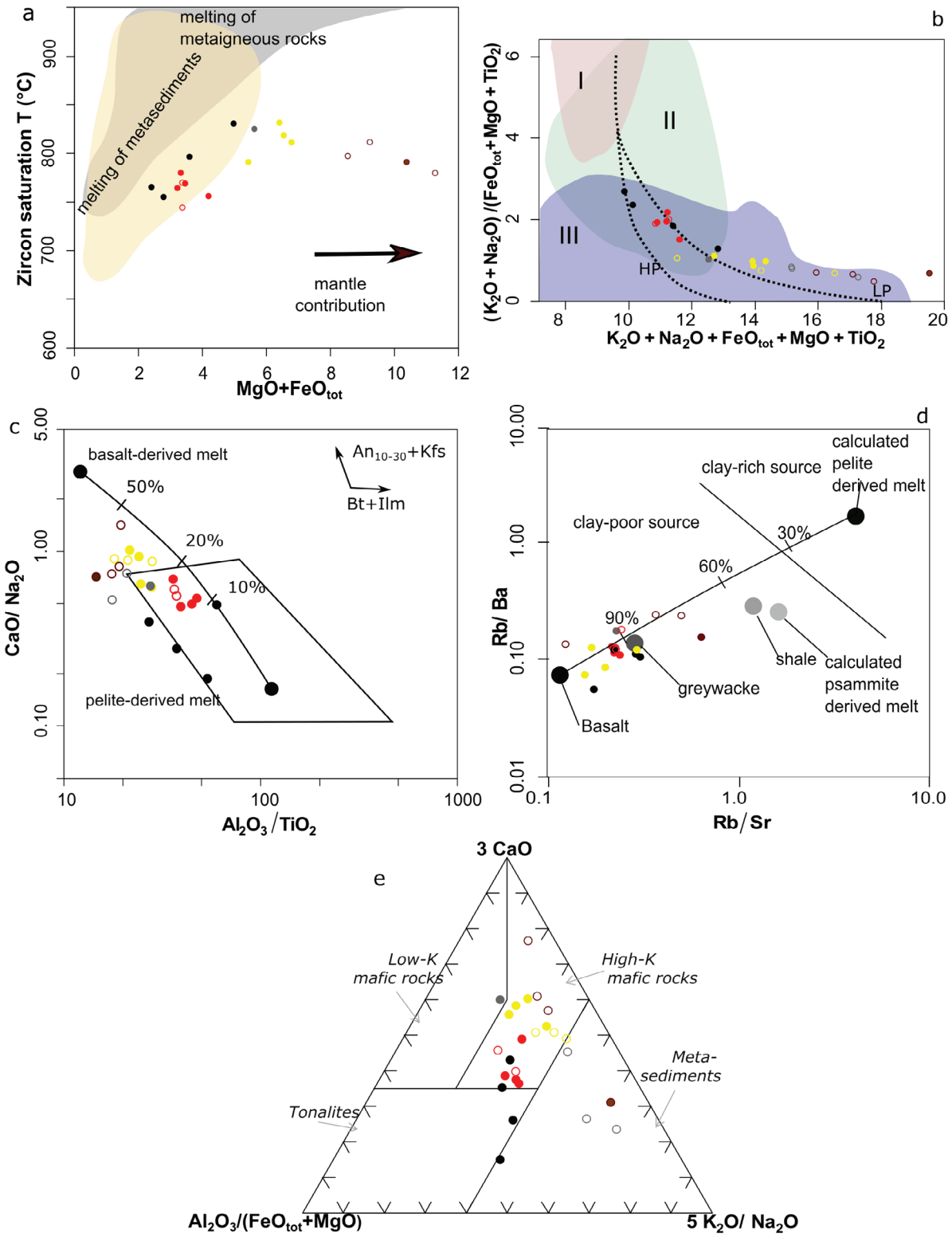

Fig. 4. Petrogenetic discrimination of LTP granitoids: **a** — Zircon saturation temperatures versus FeO_{tot}+MgO with fields plotted on the basis of compilation of melting experiments on metaigneous and metasedimentary lithologies (Laurent 2017a and references therein). **b** — $(K_2O+Na_2O)/(FeO_{tot}+MgO+TiO_2)$ vs $K_2O+Na_2O+FeO_{tot}+MgO+TiO_2$ Patiño Douce's (1999) discrimination diagram indicates different granite sources: I-metapelite II-metagreywacke III-amhibolite; black curves refer to high-pressure (HP) and low-pressure (LP) mixing between basalt and pelite-derived melt; **c** — CaO/Na_2O vs Al_2O_3/TiO_2 Patiño Douce 's (1999) discrimination diagram identifying fields from experimental melts from different sources; **d** — Sylvester's (1998) diagram with average compositions of basalt, greywacke, shale, and the hybridisation curve of basalt and pelite derived melt; **e** — Ternary source discrimination diagram on the basis of late-Archean granite chemistry (Laurent et al 2014). Symbols as on Fig. 3.

zircons are composed of multiple thin and regular growth zones (Fig 5; grains NTM:20-22_3, NTM:20-22_5, NTM:20-22_11 or NTM-12_3, NTM-12_14). Additionally, composite grains occur as well, and these zircons contain distinct cores that are morphologically different from overgrowing zones (NTM-12_4 or NTM-32(21)_11). Commonly, they are strongly corroded, cloudy, and unzoned (NTM:20-22_22; NTM-12_7). Moreover, fewer elongated, small grains <100 µm occur as well. The zircons formed from distinct generations and small grains are more common in the Prašivá *Mnz-subtype* than in the Ďumbier type and Prašivá *Aln-subtype*. A large number of zircon grains is overgrown by a homogenous, CL-dark rim indicating additional imprint.

Zircon dating results and U/Th ratio

The diatexite sample NTM-39 shows a weighted mean age of $^{206}Pb/^{238}U$ 360.4±2.7 Ma (Fig. 6a); however, some zircon recorded a younger age overgrowth between 355 and 320 Ma (4 points; SM2). The age of inherited cores is from Cambrian to Silurian periods (490–430 Ma). Analytical dating points, which yielded a time span of 380–360 Ma, show a progressively descending Th/U ratio from 1.0 to 0.01, whereas 360–320 Ma spots show a strongly variable Th/U ratio in the range of 1.1–0.3.

Zircon dating of the Ďumbier sample NTM:20-22 yielded a weighted mean age of 353.4±2.2 Ma (Fig. 6b), and the age span is generally from 360 to 340 Ma (SM2). Single inherited cores were identified as Ediacaran in age (SM2) and the Th/U ratio in these zircons shows variability from 0.13 to 1.12 with a main cluster between 0.5–0.7 (SM2).

Almost exactly the same time span is recorded in the Prašivá *Aln-subtype* zircons, which yielded an average age of 352.1 ±2.5 Ma (Fig. 6c) and cover a time span of 355–340 Ma. Two inherited cores yielded ages 419±5 Ma and 393±13 Ma; however, a few cores recorded ages around 360 Ma as well (SM2).

In contrast, zircon dating in the Prašivá *Mnz-subtype* (NTM-32) shows a more widespread range in age spots with a weighted mean age of 351.9±2.9 Ma (Fig. 6d). Application of the age unmixing Gaussian deconvolution method according to Ludwig (2009) indicates that two zircon generations are in the age of 350.6±1.5 Ma (comparable with *Aln-subtype*) and 321.7±2.1 Ma. Moreover, the outermost CL dark rims of some zircons show Permian, Triassic, and even Cretaceous age spots (SM2) with very low Th/U ratio (0.2–0.1). The morphologically-distinct zircon cores show mainly Devonian (380–365 Ma) and Ordovician ages, as well as Cambrian ages to a lesser extent.

Monazite morphology and U–Th–Pb geochronology

Monazite morphology and textural context

Monazites from migmatites often show a rounded shape, patchy zonation, and sizes up to >50 µm. Monazites are located in intra-granular position, in inclusions of biotite and plagioclase, and even within quartz inclusions encompassed in plagioclase (Fig. 7a, b). Monazite in the Prašivá *Aln-subtype* granite is almost absent, but is abundant in the *Mnz-subtype*, especially as inclusions in biotite. They show concentric zonation from the centre with often disturbed patchy or convolute zonation (Fig. 7c, d).

Monazite U–Th–Pb dating results

In NTM-39 diatexite from Jasenie monazite U–Th–Pb dating yielded an age of 348±3.0 Ma (Fig. 8a). Monazites from the sillimanite-bearing migmatite NTM:20-10 show an average age of 360±3.6 Ma; while bimodal distribution of the spot ages shows two maxima: an older at ca. 366.8±4.6 Ma and a younger at 331±11 Ma (Fig. 8b). Different age domains regularly coexist in one grain; however, their distribution is generally random.

The sample NTM-7 from the central part of the Prašivá *Mnz-subtype* intrusion shows a weighted coherent age of 351±4.1 Ma (Fig. 7c) corresponding to zircon datings of NTM-32 (Fig. 6d). The age spot data varies from the Devonian to very late Carboniferous, and their distribution shows a time span of around 60 Ma (Fig. 7c, d).

Discussion

Low Tatra granite in the frame of granites typology

Both the Ďumbier and Prašivá granitoids are peraluminous, magnesian, high-K calc-alkaline, and biotite-bearing, and differ in terms of modal composition and major element chemistry, but with similar trace element signature (compare Fig. 3a–c with 3d–f). The principal difference between the Ďumbier and Prašivá granitic rocks is in the former's more basic Ďumbier tonalitic character, which is indicated by lower SiO_2 and lower peralumosity (see Fig. 3a, b, c). The Prašivá *Aln-bearing subtype* and the Ďumbier type form a differentiation trend (e.g., Fig. 3b) similar to KCG (Bonin et al. 2020; Moyen et al. 2021), whereas the Prašivá *Mnz-bearing* subtype shows a pattern affiliated with more evolved CPG.

The absence of corroded, inherited cores in Ďumbier zonal relatively high An plagioclase points to relatively late crystallization, which along with abundant biotite and relatively high LOI (2–2.7 wt. %; SM1) imply a high water content in parental melt that formerly supressed plagioclase crystallization (Müntener et al. 2001). Brittle deformation of plagioclase phenocrysts (Fig. 2e) and kinking of biotite laths, as well as anisotropic fabric are observed in marginal parts of the pluton (Fig. 2c; Siegl 1970) and can be interpreted as a deformation at the suprasolidus stage (Paterson et al. 1998; Vernon et al. 2004) during new pulses of magma.

In comparison to the Ďumbier tonalite/granodiorite, the Prašivá granodiorites–granites show more pronounced compositional heterogeneity related to mixing (Maraszewska et al. 2019a). Allanite and monazite stability is governed by pT

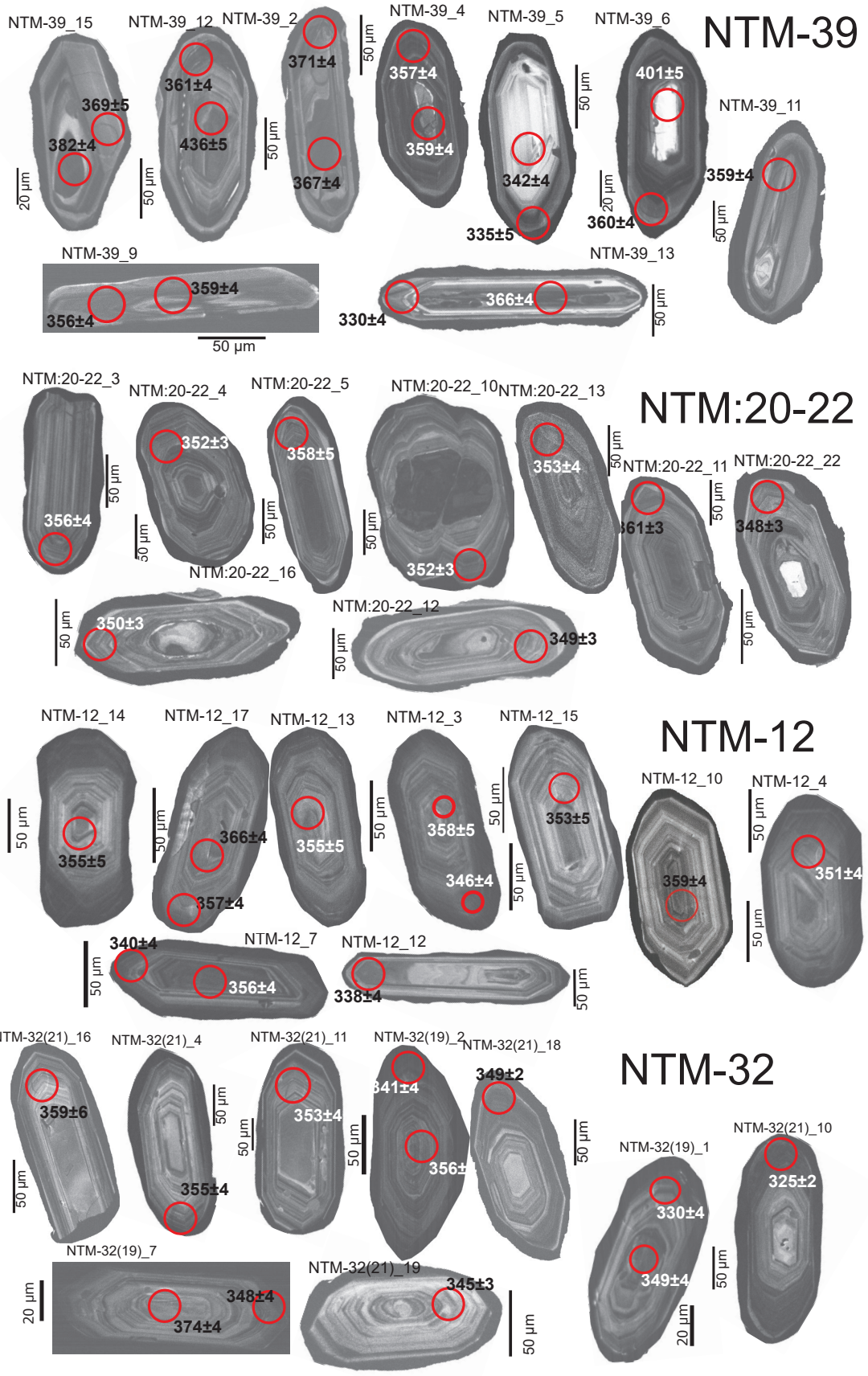

Fig. 5. Representative CL images of dated zircons with analytical points and common Pb corrected spot ages. The NTM-32 zircons numbers in brackets after each sample's name refers to the mound analysed in 2019 and 2021, respectively)

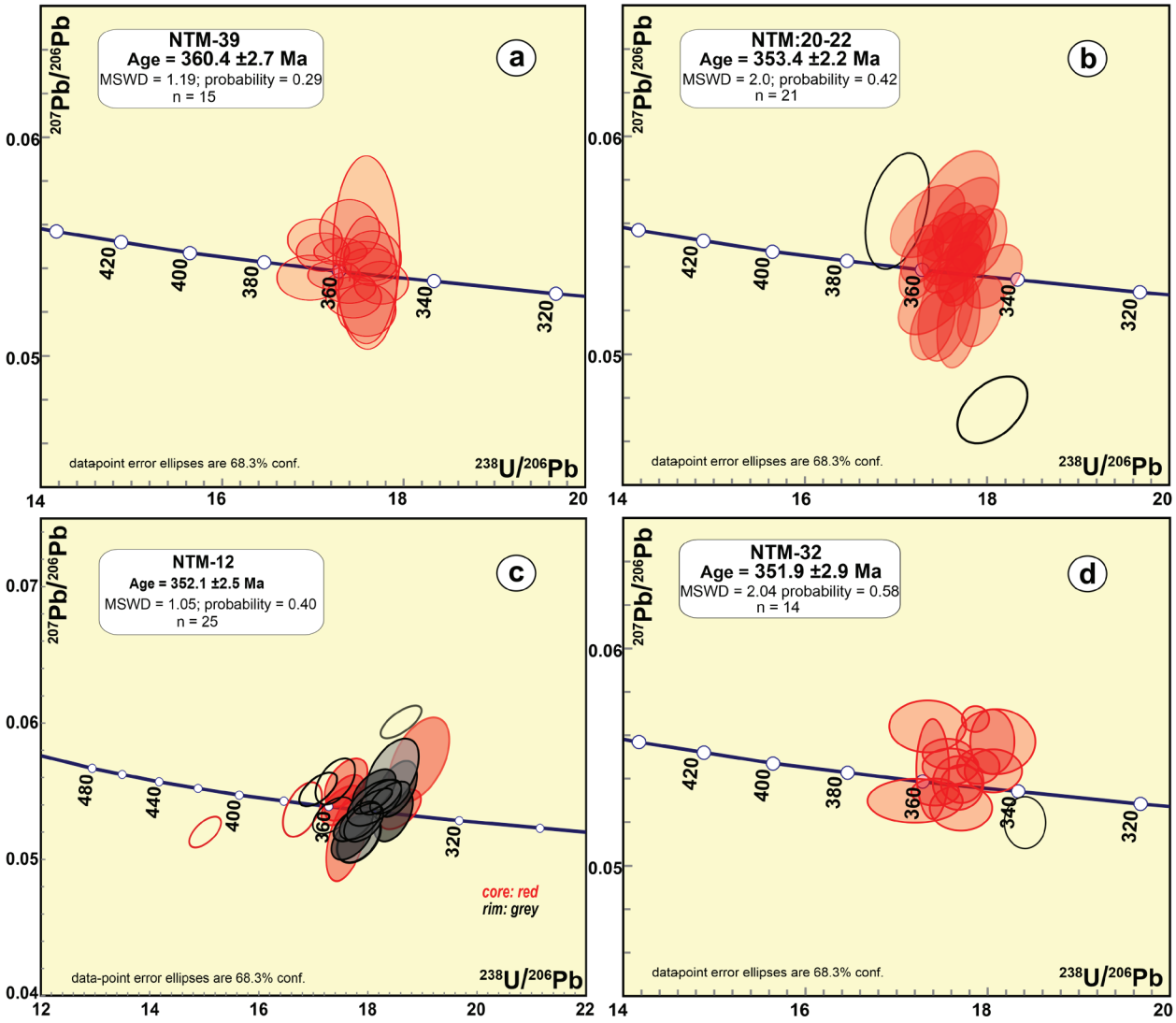

Fig. 6. SHRIMP concordia plots of zircon datings. **a** — Tonalitic diatexite; **b** — Ďumbier type; **c** — Aln-Prašivá subtype; **d** — Mnz-Prašivá subtype.

magma conditions and Ca content, which is in turn strongly controlled by the hybridisation process (e.g., Dini et al. 2004). The hybrid nature of the Prašivá types documents the presence of amphibole–biotite-rich dioritic enclaves consumed during mixing (Poller et al. 2005), as well as Ca-rich cores in plagioclase and K-feldspar porphyrocrysts with variable, but always cocentric zonation BaO patterns (e.g., Słaby et al. 2007), which encloses plagioclase oriented parralel to growth zones (Fig. 2g). In the microgranular mafic enclaves, magma–magma interaction (magma mixing) is evidenced by preserved oscillatory zonation of Ca in plagioclase (Fig. 2k) and the presence of quartz ocelli's (Fig. 2j). However, high-Ca patchy cores in plagioclase in the Prašivá subtypes show nearly the same anorthite content as in the plagioclase from the Ďumbier type giving them to one magmatic suite. Moreover, the marginal facies of the Ďumbier type sometimes include sporadic K-feldspar megacrysts.

The Prašivá *Aln-subtype* shows coherent trends in terms of the major elements, showing stronger affinity to KCG, whereas the chemical compositions of the Prašivá *Mnz-subtype* are much more variable and resemble the evolved granites towards the CPG (Laurent et al. 2017a; Bonin et al. 2020; Fig. 3b). Isotope studies from the Liptovská Lúžna area (the Prašivá *Aln-subtype*) show a low $^{87}Sr/^{86}Sr_{(0)}$ ranging between 0.70876–0.71010 (Kohút et al. 1999; Poller et al. 2005; Kohút & Nabelek 2008), which corresponds to a lower crustal ± mantle source with minor contribution of upper crustal magmas. However, the Prašivá *Mnz-bearing* subtype from the SE part of LTP shows increased radiogenic Sr ($^{87}Sr/^{86}Sr_{(0)}$ = 0.7123–0.7150; Bagdasaryan et al. 1985) indicating higher contribution of crustal material. These differences are also emphasised by the source discrimination diagrams of Patiño Douce (1999), Sylvester (1998), and Laurent et al. (2014) (Fig. 4b–e), which clearly indicate stronger affinity of

Aln-subtype to mafic or intermediate sources, and *Mnz-subtype* to metasedimentary or felsic metaigneous source.

Post-collisional granite setting

Contrary to the contrasting textures and major element composition, the trace element content and REE patterns are similar for both the Ďumbier and Prašivá granitic types. They are characterised by high REE and strong LREE/HREE fractionation (Fig. 3d), high Ba, Sr, and moderate Rb contents (Fig. 3e) like in the granites with I- type affinity. One very distinctive feature is high Sr/Y and La/Yb ratios, which is typical for "adakitic" or "sanukitoid-like" melts (Moyen 2009). Positions of the studied samples in the Patiño Douce (1999) and Laurent et al. (2014) discrimination diagrams are consistent with the derivation of Bt-granitoids in the LTP from a mixed mafic metaigneous and metasedimentary source, with increasing volume proportion of the "crustal" magmas along the line Ďumbier–*Aln*-Prašivá–*Mnz*-Prašivá evolution. However, zircon saturation temperatures are much lower than is generally expected for dehydration melting of metaigneous lithologies >900 °C (Fig. 4a; Rapp & Watson 1995; Skjerlie & Patiño Douce 2002), which can suggest a water-fluxed melting process that can be initiated at T = 850–900 °C (Beard & Lofgren 1991; Collins et al. 2016).

The trace element signatures of the Prašivá and the Ďumbier type reflect the chemistry of arc granite (Pearce et al. 1984), and such a setting has already been proposed by Petrík (2000) and Poller et al. (2005). However, this model can be misleading, since subduction signature can be inherited either from a mantle metasomatized component from slab-derived fluids (Zhao et al. 2013) or from intermediate granulite residue in a post-collisional setting (Castro 2020). Moreover, it can be inherited from remelting of pre-existing arc-related mafic to intermediate magmas (Frost & Frost 2008). The high-K, Ba, Sr, and LREE detected in LTP is a typical characteristic feature of the post-collisional Caledonian granites in classic localities like Scotland and Ireland (Atherton & Ghani 2002; Ghani & Atherton 2008) or within the Pan-African suites of the Tuareg shield (Liégeois et al. 1998).

Adakitic signatures in granites

Sanukitoid or adakite-like signature in the LTP granites identified typical Sr/Y and La/Yb ratio characteristics, which originated from the lower crustal protolith by enriched mantle-related magma (Guo et al. 2007). In European Variscides, high K, Sr, Ba, and LREE characteristics of granitoids are from mantle-related high K-Mg and LILE magmas (e.g., Moyen et al. 2017). The composition of the LTP seems to be formed by fractionation of phases with high Y+HREE mineral/melt partition coefficients (e.g., Xu et al. 2015; Kendrick & Yakymchuk 2020) like garnet or amphibole present. The fractionation of HREE-bearing phases indicates steep chondrite-normalised patterns in LTP granitoids (Fig. 3d). Melting experiments performed on basic to intermediate

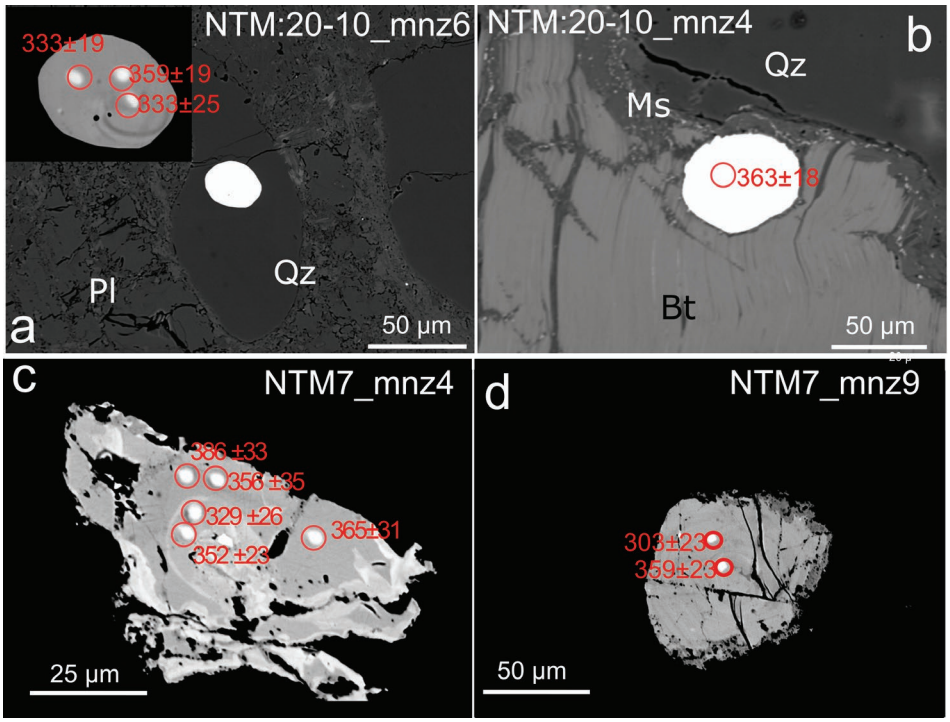

Fig. 7. Representative BSE microphotographs showing analytical spots in selected dated monazite grains and their textural context. **a, b** — Migmatite – note the rounded morphology typical for monazite in migmatite; **c** — Large, complex zoned monazite hosted by biotite in the Mnz-subtype Prašivá (Magurka): note the coexistence of different age domains without clear structural pattern; **d** — concentrically-zoned subhedral monazite hosted by biotite in the Mnz-subtype Prašivá.

lithologies show that the melts in water-present conditions at pressure <5 kbar in equilibrium with amphiboles are peraluminous with a high K/Na ratio, whereas fractionation of peritectic garnet under higher pressures produces lower-alumina melts (Zen 1986; Alonso-Perez et al. 2009; Bucholz et al. 2014). The saturation of the magmatic system by volatiles stabilises amphiboles instead of its consumption via dehydratation-melting (Weinberg & Hasalová 2015; Johnson et al. 2021). Peritectic hornblende usually forms along with plagioclase, which buffers the Sr content of melt (Moyen 2009); however, the high-water content under HP conditions suppresses crystallisation of plagioclase (Alonso-Perez et al. 2009; Kolb et al. 2013). More pronounced "adakitic" signature and lower Dy/Yb ratios (Davidson et al. 2012) observed in the Prašivá granite types along with its more felsic character in comparison to the Ďumbier type can reflect the lower incorporation of peritectic amphibole into partial melt products due to lower temperatures or higher pressures of melting (Alonso-Perez et al. 2009). Inheritance of high Sr/Y and La/Yb from an intermediate metaigneous source, which could be an equivalent of TTG, is unlikely because the partial melting of TTG's does not produce high-K magmas (Watkins et al. 2007). The relatively lower Sr/Y ratio in the enclaves can be explained by the higher mobility of Sr against Y (Laurent et al. 2017b) or higher temperatures exceeding the upper stability limit of peritectic amphibole (Alonso-Perez et al. 2009; Castro et al. 2010; Rodríguez et al. 2019).

Interpretation of Tournaisian zircon and monazite geochronology

The average zircon age ca. 360 Ma of diatexite (Fig. 6a; SM2) is interpreted as a high-T metamorphic anatectic age formed during decompression. In the Western Tatra Mts., the similar ages between 360–355 Ma of migmatites and orthogneisses (Poller et al. 2000) are interpreted as the timing of high-grade syn-collisional metamorphism followed by extensive anatexis. Such ages recorded in inherited monazite from the Jasenie leucogranite (Petrík & Konečný 2009) were interpreted as metamorphic. Dating of diatexites in the Malá Fatra Mts. yielded an age of 362 Ma (Broska et al. 2022) close to the age of the Low Tatra diatexites. The lower monazite ages of tonalitic diatexite (348 Ma) can be interpreted as an imprint age from decompression-driven anataxis or from influence of a contact younger melt (Fig. 8a; SM3). The two tectonothermal events are recorded in bimodal ages in sillimanite-bearing migmatite, with the older one ca. 366 Ma and the younger ca. 331 Ma (Fig. 8b; SM3). The age of ca. 345–340 Ma recorded in retrogressed eclogites and migmatites of the Western Tatra Mts. is linked with rapid extrusion of lower crustal lithology driven by extensional forces and culmination of crustal anatexis (Moussallam et al. 2012). However, the younger ages are relatively rare in zircon rims (Figs. 5, 6a; SM2) and can indicate the growth of zircon in lower temperature conditions and a water-fluxed regime in the frame of a decompressional anatectic event (Couzinié et al. 2021), or tectono-thermal imprint connected with decompression.

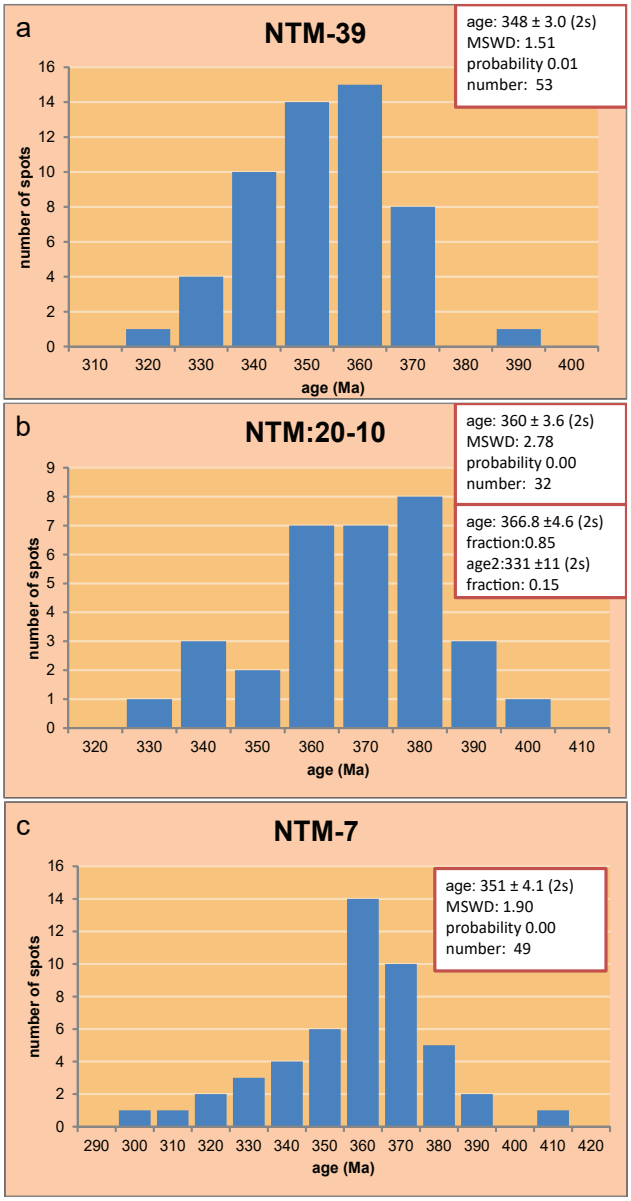

Fig. 8. U–Th–Pb monazite weighted average age. **a** — Granodioritic diatatexite, Jasenie; **b** — Sil-bearing stromatitic migmatite, block within Ďumbier granite, Skalka area; **c** — Mnz-subtype Prašivá, Magurka mining district.

The Ďumbier sample NTM:20-22 yielded an age of 353.4 ±2.2 Ma. Dating performed on the Ďumbier type by Broska et al. (2013) showed an age ca. 356 Ma; however, datings of Ďumbier granitoids presented by Kohút & Larionov (2021) and previously by Putiš et al. (2003) yielded much younger ages of 340 and 343 Ma, respectively, which the authors interpreting them as collisional event. The sequence ages of 353–351 Ma for the Prašivá type (*Aln-subtype* variety and *Mnz-subt*ypes; Fig. 6c and d) supported by Tournaisian dating ca. 353 Ma published by Broska et al. (2013) seems to be

a record of the main magmatic activity in the area. Nevertheless, individual age spots recorded in zircons from the Ďumbier and Prašivá granitoids also show a wide interval between 360–345 Ma (Figs. 5 and 6b, c, d; SM2), thereby reflecting the long growth of the pluton formed via consumption and recycling of more pre-existing mafic portions of magmas by new fluxes of magma progressively enriched in a "crustal" component (Maraszewska et al. 2019b). Zircon dating of diorite in the Malé Železné Valley, which yielded an age of 354±6.8 Ma (Spišiak et al. 2017), indicates the expectation that intermediate magmas preceeded the main Variscan granitic magmatism. On the other hand, the age evolutionary sequence deconstructs the published "young" age of the diorite body from the Bor peak at 350±2 Ma (Uher et al. 2011) needs further detail inspection in the future. Our data support the long-termed evolution from the lower Tournaisian formation of LTP granitoids, which had evolved from tonalite to granite facies over time.

While the average age sequence from 353 Ma old Ďumbier granite to 352 Ma for the Prašivá *Aln-subtype*, and 351 Ma for the Prašivá *Mnz-subtype* suggests a nearly coeval time of partial melting of different lower- and middle crustal lithologies, the magmatic products resulted in geochemical differences of principal granite types. Clearly visible magma–magma interaction in the time period of ca. 3 Myr, which was documented by the flow of textures of unconsolidated crystals in marginal facies of the Ďumbier area, includes widespread brecciation of plagioclase phenocrysts that are typical for sequential emplacement of multiple pulses of magma (e.g., in the Strzelin massif, see Oberc-Dziedzic et al. 2013), despite that the typical sequential emplacement is a widely accepted model for zonal plutons (Glazner et al. 2004; Miller et al. 2011). Inherited zircon grains in the Ďumbier and Prašivá granitoids (500–400 Ma) generally cover the ages of protolith of orthogneisses and metabasites, thus indicating contribution from the Cambrian–Ordovician crust (Putiš et al. 2008, 2009).

Pennsylvanian and post-Variscan record in granitic rocks

The age spots in zircons in the *Mnz-subtype* of the Prašivá indicate the late magmatic processes at an age of ca. 330–320 Ma. The first possibility is that the Pennsylvanian ages reflect its re-equilibration and re-growth triggered by reheating and fluid circulation during decompression (Vavra et al. 1996). The possible mechanism responsible for disturbance in zircons isotope systematics is extensive annealing and damage of the zircon structure, which is supported by the strain and defects in zircon (Schaltegger et al. 1999). Microprobe analysis of zircons reveals that the rims of zircons or entire grains in the Prašivá quite often contain elevated Y+HREE (up to 4 wt.%) and P (up to 3 wt.%), which explains their susceptibility to damage. Moreover, the sample NTM-32 was taken close to a leucogranite body, whose emplacement could have thermally affected the zircons (Fig. 1). Consequently, the Pennsylvanian dates in zircons are likely connected with zircon overprint during uplift and associated fluid circulation.

The Permian ages that frequently occur in the leucogranite zircon rims in the current area of the Western Carpathians resulted from emplacement of post-orogenic and anorogenic bimodal magmatism related to continental rifting and the opening of the Neo-Tethys Basin (Ondrejka et al. 2018, 2021; Villaseñor et al. 2021). The Permian activity is proven by dykes of lamprophyres in the Low Tatra Mts. area, as well as crosscutting granitoids and orthogneisses at an age of ca. 260 Ma (Spišiak et al. 2018, 2021). Subsequent extensive heating and fluid circulation in the crust can cause Pb-loss from recrystallized zircon rims (e.g., Geisler et al. 2007), as well as metasomatic dissolution and re-precipitation of apatite and secondary monazite formation. Alpine ages constrained in some zircon rims reflect Pb-loss during Mesozoic reworking of the crystalline basement and arrangement in current tectonics.

Proposed geodynamic scenario

The crucial controversy in modelling of the crustal melting concerns the source of heat (e.g., Moyen et al. 2021), because underplated mafic mantle magmas cannot trigger voluminous crustal magmatism. A revisited model of the late Devonian/early Carboniferous geodynamics in the Western Carpathian segment of the Variscides was discussed, highlighting the role of slab breakoff based on the model of Davies and von Blanckenburg (1995), which had been recognised also in the Malá Fatra Mts. (Broska et al. 2022). This model is plausible and explains the delivery of sufficient heat to the re-melting layered crust due to delamination of subducted crust and rapid decompression that caused melting of the overlying crust. There are numerous typical features of such mechanisms, e.g., exposures of deep, continental, crust roots as gneiss-dominated high-grade metamorphic complexes with lenses of high-pressure rocks as eclogites and mantle xenoliths, intruded by bimodal magmatism representing various magma sources (Davies & von Blanckenburg 1995).

The geochronological time scale of granitoid production in the LTP cannot be treated as an isolated body, since all core complexes in the Tatric massifs are part of one orogenic system. The process of Devonian deep crustal subduction is evidenced by the presence of the retrogressed eclogites in the Western Tatra Mts. (Janák et al. 1996; Janák 2019, Burda et al. 2021). Retrogressed eclogites, which indicate HP metamorphism (minimum pressure 15–16 kbar; e.g., Janák et al. 1996; Janák 2019), were recently studied by means of zircon dating (Burda et al. 2021). Obtained zircon data at ca. 367 Ma were interpreted as an HP event, which was followed by amphibolite-facies retrograde metamorphism at ca. 349 Ma (Burda et al. 2021). According to Moussallam et al. (2012), eclogites in the Baranec area were subducted to a depth of 45 km (P=15 kbar) together with hosting migmatites (12 kbar) and the analogous eclogites described in the Malá Fatra Mts. (Janák & Lupták 1997). It must be noted that similar retro-

gressed eclogites like the ones hosted in the Upper Unit (the Western Tatra Mts.) were described in the Low Tatra Mts. as well, in very similar metamorphic granulite-facies conditions 750–760 °C and 11–15 kbar (Janák et al. 2009). The presence of eclogites, which were hosted in the high-grade crustal lithology, is crucial evidence of deep continental subduction. The late-stage process of subduction was also connected with magmatic activity and the formation of the calc alkaline metaluminous arc-related diorites in the Tatra Mts., as well as their hybrids with crustal magmas (Burda et al. 2011; Gaweda et al. 2016; Broska et al. 2022). If the peak of subduction-collision metamorphism occurred at ca. 370–360 Ma, the ages constrained for the Ďumbier and Prašivá granitoids at ca. 353–351 Ma point to a post-collisional phase and chemical affiliation with 'Caledonian type of batholiths' (Ghani & Atherton 2008). The time span between the collision and generation of post-collisional suites could be over 30 Myr, although syn-collisional slab break off could have significantly reduced that gap to only a few million years (Hildebrand & Whalen 2014). The mantle upwelling enhanced by slab break off caused a flux of hot mantle material, as well as low degree water-saturated partial melting of deep roots of the continental crust. Involvement of the mantle material was proposed by Poller et al. (2005) in the genesis of the Prašivá type and its enclaves. However, post-collisional suites dominated by derivatives from juvenile mantle material are characterised by high proportions of intermediate and mafic lithologies (e.g., Clemens et al. 2009; Fiannacca et al. 2015), whereas in the LTP, diorites preserved as small bodies, and the LTP massif generally lacks any contemporaneous gabbros or ultramafic cumulates. As a consequence, the mantle diapir likely served as a source of heat and volatiles required for extensive melting of the lower crust, but its mixing/mingling with lower crustal magmas was negligible, which was documented by the relatively evolved δ^7Li and $^{87}Sr/^{86}Sr_{(i)}$ isotope composition of diorites (Magna et al. 2010). Therefore, it is possible that the mafic to intermediate source was formed by previous subduction-related enriched mantle-derived high-K, and high in Ba, Sr, Sr/Y, and LREE magmas, underplating continental arc crust. Detachment of the subducted slab would have caused significant density loss and buoyancy-driven rapid elevation of the lower crustal zones, which were supported by radiogenic heating, shearing, and heat, including the volatile supply from mafic magmas, which triggered lower pressure anatexis of heterogeneous crustal lithologies (Gerbi et al. 2006; Dokuz 2011). This would have thus resulted in the evolution of various magmatic series from dioritic to subaluminous tonalitic, and to subsequent intrusion of peraluminous granodioritic–granitic magmas.

Conclusions

The composite Low Tatra pluton is related to post-collisional late-Variscan magmatism involving the previous partial melting of various lower crustal lithologies. The geodynamic regime operated from subduction and collision-related metamorphism with decompressional anatectic melting at 360 Ma, and the detachment of the subducted slab led to the subsequent extraction of calc-alkaline high-K magmas from mafic lower crustal sources, which had been heated and melted by mantle upwelling. The former I-type magmas were progressively mixed with later magmas derived from sedimentary and/or metagranitic sources, giving the melts a more "crustal", CPG character. Such melting is proposed during post-collisional extension and rapid uplift. Thus, the interplay of various melting/differentiation processes evolving over time at sufficient P–T conditions with peritectic/restitic phase's entrainment, magma hybridisation, and accumulation/fractionation, shaped a composite character of the Low Tatra pluton. The protracted evolution of these granitoids, as well as the effect of mantle-related volatiles could have also contributed to rich polymetallic ore mineralisation, since molybdenite in highest-temperature metal association was dated at 351 Ma by the Re–Os method, and S and O isotopes, as well as fluid inclusion studies pointed to endogenic sources of ore fluids (Majzlan et al. 2020a, b and references therein).

Acknowledgements: Support from the Slovak Research and Development Agency: APVV-18-0107, VEGA 2/0075/20 and bilateral grant APVV SK-KR-18-0008 are greatly appreciated. We thank Martin Ondrejka and Magdalena Pańczyk-Nawrocka for their constructive comments that helped to improve the original manuscript, as well as Katarína Bónová for editorial handling. We also thank Michael Sabo for his proofreading of the English text.

References

Alonso-Perez R., Müntener O. & Ulmer P. 2009: Igneous garnet and amphibole fractionation in the roots of island arcs: experimental constraints on andesitic liquids. *Contributions to Mineralogy and Petrology* 157, 541–558. https://doi.org/10.1007/s00410-008-0351-8

Atherton M.P. & Ghani A.A. 2002: Slab Breakoff: A Model for Caledonian, Late Granite Syn–Collisional Magmatism in the Orthotectonic (Metamorphic) Zone of Scotland and Donegal, Ireland. *Lithos* 62, 65–85 . https://doi.org/10.1016/S0024-4937(02)00111-1

Bagdasaryan G.P., Gukasyan R.Kh., Cambel B. & Veselský J. 1985: Rb–Sr isochron dating of the Ďumbier zone granitoids of the Nízke Tatry Mts. (Western Carpathians). *Geologický Zborník Geologica Carpathica* 36, 637–645.

Barbarin B. 1990: Granitoids: main petrogenetic classifications in relation to origin and tectonic setting. *Geological Journal* 25, 227–238. https://doi.org/10. 1002/gj.3350250306

Barbarin B. 1999: A review of the relationships between granitoid types, their origins and their geodynamic environments. *Lithos* 46, 605–626. https://doi.org/10.1016/S0024–4937(98)00085–1

Baxter S. & Feely M. 2002: Magma mixing and mingling textures in granitoids: examples from the Galway Granite, Connemara, Ireland. *Mineralogy and Petrology* 76, 63–74. https://doi.org/10.1007/s007100200032

Beard J.S. & Lofgren G.E. 1991: Dehydration melting and water–saturated melting of basaltic and andesitic greenstones and amphibolites at 1, 3, and 6.9 kb. *Journal of Petrology* 32, 365–401. https://doi.org/10.1093/petrology/32.2.365

Biely A. (Ed.) Beňuška P., Bezák V., Bujnovský A., Halouzka R., Ivanička J., Kohút M., Klinec A., Lukáčik E., Maglay J., Miko O., Pulec M., Putiš M. & Vozár J. 1992: Geological map of the Nízke Tatry Mts. 1:50,000. *Dionýz Štúr Institute of Geology*, Bratislava.

Boehnke P., Watson E. B., Trail D., Harrison T. M. & Schmitt A. K. 2013: Zircon saturation re-revisited. *Chemical Geology* 351, 324–334. https://doi.org/10.1016/j.chemgeo.2013.05.028

Bonin B., Janoušek V. & Moyen J.F. 2020: Chemical variation, modal composition and classification of granitoids. In: Janoušek V., Bonin B., Collins W.J., Farina F. & Bowden P. (Eds.): Post–Archean Granitic Rocks: Petrogenetic Processes and Tectonic Environments. *Geological Society of London Special Publications* 491, 9–51. https://doi.org/10.1144/SP491-2019-138

Boynton W.V. 1984: Cosmochemistry of the rare earth elements meteorite studies. In: Henderson P. (Ed.): Rare Earth Element Geochemistry. *Elsevier.* Amsterdam, 63–114

Broska I. & Petrík I. 1993: Magmatic enclaves in granitic rocks of the Western Carpathians. *Mineralia Slovaca* 25, 104–108.

Broska I. & Uher P. 1991: Regional typology of zircon and their relationship to allanite–monazite antagonism on example of Hercynian granitoids of the Western Carpathians. *Geologica Carpathica* 42, 271–277.

Broska I. & Uher P. 2001: Whole–rock chemistry and genetic typology of the West–Carpathian Variscan granites. *Geologica Carpathica* 52, 79– 90.

Broska I., Petrík I. & Benko P. 1997: Petrology of the Malá Fatra granitoid rocks (Western Carpathians, Slovakia). *Geologica Carpathica* 48, 27–37

Broska I., Petrík I., Be'eri–Shlevin Y., Majka J.& Bezák V. 2013: Devonian/Mississippian I–type granitoids in the Western Carpathians: A subduction–related hybrid magmatism. *Lithos* 162–163, 27–36. https://doi.org/10.1016/j.lithos.2012.12.014

Broska I., Janák M., Svojtka M., Yi K., Konečný P., Kubiš M., Kurylo S., Hrdlička M. & Maraszewska M. 2022: Variscan granitic magmatism in the Western Carpathians with linkage to slab break–off. *Lithos* 412–413, 106589. https://doi.org/10.1016/j.lithos.2021.106589

Bucholz C.E., Jagoutz O., Schmidt M.W. & Sambuu O. 2014: Fractional crystallization of high–K arc magmas: biotite- versus amphibole-dominated fractionation series in the Dariv Igneous Complex, Western Mongolia. *Contributions to Mineralogy and Petrology* 168, 1–28. https://doi.org/10.1007/s00410-014-1072-9

Burda J., Gawęda A. & Klötzli U. 2011: Magma hybridization in the Western Tatra Mts. granitoid intrusion (S–Poland, Western Carpathians). *Mineralogy and Petrology* 103, 19–36. https://doi.org/10.1007/s00710–011–0150–1

Burda J., Klötzli U., Woskowicz–Ślęzak B., Li Q.L. & Liu Y. 2020: Inherited or not inherited: Complexities in dating the atypical 'cold' Chopok granite (Nízke Tatry Mountains, Slovakia). *Gondwana Research* 87, 138–161. https://doi.org/10.1016/j.gr.2020.05.018

Burda J., Klötzli U., Majka J., Chew D., Li Q–L., Liu Y., Gawęda A. & Wiedenbeck M. 2021: Tracing proto–Rheic–Qaidam Ocean vestiges into the Western Tatra Mountains and implications for the Palaeozoic palaeogeography of Central Europe. *Gondwana Research* 91, 188–204. https://doi.org/10.1016/j.gr.2020.12.016

Castro A. 2020: The dual origin of I–type granites: the contribution from experiments. In: Janoušek V., Bonin B., Collins W.J., Farina F., Bowden P. (Eds.): Post–Archean Granitic Rocks: Petrogenetic Processes and Tectonic Environments. *Geological Society of London Special Publications* 491, 101–145. https://doi.org/10.1144/SP491–2018–110

Castro A., Gerya T., García–Casco A., Fernández C., Díaz–Alvarado J., Moreno–Ventas I. & Löw I. 2010: Melting relations of MORB–sediment mélanges in underplated mantle wedge plumes; implications for the origin of Cordilleran–type batholiths. *Journal of Petrology* 51, 1267–1295. https://doi.org/10.1093/petrology/egq019

Chappell B.W. & White A.J.R. 1974: Two contrasting granite types. *Pacific Geology* 8, 173–174.

Chovan M., Slavkay M. & Michálek J. 1996: Ore mineralization of the Ďumbierske Tatry Mts. (Western Carpathians, Slovakia). *Geologica Carpathica* 47, 371–382.

Clemens J.D., Darbyshire D.P.F. & Flinders, J. 2009: Sources of post-orogenic calcalkaline magmas : the Arrochar and Garabal Hill–Glen Fyne complexes, Scotland. *Lithos* 112, 524–542. https://doi.org/10.1016/j.lithos.2009.03.026

Collins W.J., Huang H.–Q.& Jiang X. 2016: Water–fluxed crustal melting produces Cordilleran batholiths. *Geology* 44, 143–146. https://doi.org/10.1130/G37398.1

Couzinié S., Bouilhol P., Laurent O., Marko L. & Moyen J. M. 2021: When zircon drowns: Elusive geochronological record of water-fluxed orthogneiss melting in the Velay dome (Massif Central, France). *Lithos* 384, 105938. https://doi.org/10.1016/j.lithos.2020.105938

Davidson J., Turner S. & Plank T. 2012: Dy/Dy*: Variations Arising from Mantle Sources and Petrogenetic Processes. *Journal of Petrology* 54, 525–537. https://doi.org/10.1093/petrology/egs076

Dini A., Rocchi S. & Westerman D.S. 2004: Reaction microtextures of REE–Y–Th_u accessory minerals in Monte Capanne pluton (elba Island, Italy): possible indicator of hybridisation processes. *Lithos* 78, 101–118. https://doi.org/10.1016/j.lithos.2004.04.045

Davies J.H. & von Blanckenburg F. 1995: Slab breakoff: A model of lithosphere detachment and its test in the magmatism and deformation of collisional orogens. *Earth and Planetary Science Letters* 129, 85–102. https://doi.org/10.1016/0012–821X(94)00237–S

De la Roche H., Leterrier J., Grandclaude P. & Marchal M. 1980: A Classification of Volcanic and Plutonic Rocks Using R1–R2 Diagrams and Major Element Analyses – Its Relationships with Current Nomenclature. *Chemical Geology* 29, 183–210. https://doi.org/10.1016/0009–2541(80)90020–0

Defant M.J. & Drummond M.S. 1990: Derivation of some modern arc magmas by melting of young subducted lithosphere. *Nature* 347, 662–665. https://doi.org/10.1038/347662a0

Dokuz A. 2011: Slab detachment and delamination model for the generation of Carboniferous high–potassium I–type magmatism in the Eastern Pontides, NE Turkey: The Köse composite pluton. *Gondwana Research* 19, 926–944. https://doi.org/10.1016/j.gr.2010.09.006

Dupej J. & Siegl K. 1984: Geology of the Králička granite and its environment Nízke Tatry Mts, Western Carpathians. *Geologica Carpathica* 35, 395–411.

Fiannacca P., Cirrincione R., Bonanno F.& Carciotto M.M. 2015: Source–inherited compositional diversity in granite batholiths: the geochemical message of Late Paleozoic intrusive magmatism in central Calabria (southern Italy). *Lithos* 236, 123–140. https://doi.org/10.1016/j.lithos.2015.09.003

Finger F., Roberts M., Haunschmid B., Schermaier A. & Steyrer H. 1997: Variscan granitoids of central Europe: Their typology, potential sources and tectonothermal relations. *Mineralogy and Petrology* 61, 67–96. https://doi.org/10.1007/BF01172478

Frost B.R.& Frost C.D. 2008:A Geochemical Classification for Feldspathic Igneous Rocks. *Journal of Petrology* 49, 1955–1969,

Frost B.R., Barnes C.G., Collins W.J., Arculus R.J., Ellis D.J. & Frost C.D. 2001: A geochemical classification for granitic rocks. *Journal of Petrology* 42, 2033–2048. https://doi.org/10.1093/petrology/egn054

Gawęda A., Burda J., Klötzli U., Golonka J. & Szopa K. 2016: Episodic construction of the Tatra granitoid intrusion (Central Western Carpathians, Poland/Slovakia): consequences for the geodynamics of Variscan collision and Rheic Ocean closure. *International Journal of Earth Sciences* 105, 1153–1174. https://doi.org/10.1007/s00531–015–1239–2

Geisler T., Schaltegger U. & Tomaschek F. 2007: Re–equilibration of zircon in aqueous fluids and melts. *Elements* 3, 43–50. https://doi.org/10.2113/gselements.3.1.43

Gerbi C.C., Johnson S.E. & Koons P.O. 2006: Controls of low–pressure anatexis. *Journal of Metamorphic Petrology* 24, 107–118. https://doi.org/10.1111/j.1525-1314.2005.00628.x

Ghani A.B.& Atherton M.P. 2008: The chemical character of the Late Caledonian Donegal Granites, Ireland, with comments on their genesis. *Transactions of the Royal Society of Edinburgh: Earth Sciences* 97, 437–454. https://doi.org/10.1017/S0263593300001553

Glazner A.F., Bartley J.M., Coleman D.S., Gray W.& Taylor R.Z. 2004: Are plutons assembled over millions of years by amalgamation from small magma chambers? *GSA Today* 14, 4–11. https://doi.org/10.1130/1052-5173(2004)014<0004:APAOMO->2.0.CO;2

Guo F., Nakamuru E., Fan W., Kobayoshi K. & Li C. 2007: Generation of Palaeocene Adakitic Andesites by Magma Mixing; Yanji Area, NE China. *Journal of Petrology* 48, 661–692. https://doi.org/10.1093/petrology/egl077

Hibbard M.J. 1981: The magma mixing and origin of mantled feldspars. *Contributions to Mineralogy and Petrology* 76, 158–170. https://doi.org/10.1007/BF00371956

Hildebrand R.S. & Whalen J.B. 2014: Arc and slab–failure magmatism in Cordilleran batholiths II – the Cretaceous Peninsular Ranges Batholith of southern Baja California. *Geoscience Canada* 41, 399–458.

Hovorka D. & Méres Š. 1997: Geochemistry of the Early Paleozoic felsic metavolcanics of the Gemeric unit (Western Carpathians). In: Grecula P., Hovorka D. & Putiš M. (Eds.): Geological Evolution of the Western Carpathians. *Mineralia Slovaca – Monograph*, Bratislava, 289–300.

Jacob J.–B., Moyen J.–F., Fiannacca P., Laurent O., Bachmann O., Janoušek V., Farina F. & Villaros A. 2021: Crustal melting vs. fractionation of basaltic magmas: Part 2, Attempting to quantify mantle and crust contributions in granitoids. *Lithos* 402–403, 106292. https://doi.org/10.1016/j.lithos.2021.106292

Janák M. 2019: Eclogites of the Western Carpathians revisited. In: Proceedings of the Geologica Carpathica 70 Conference. Bratislava, 69–70.

Janák M. & Lupták B. 1997: Pressure–temperature conditions of high–grade metamorphism and migmatitization in the Malá Fatra crystalline complex, the Western Carpathians. *Geologica Carpathica* 48, 287–302.

Janák M., O'Brien P.J., Hurai V. & Reutel C. 1996: Metamorphic evolution and fluid composition of garnet–clinopyroxene amphibolites from the Tatra Mountains, Western Carpathians. *Lithos* 39, 57–79. https://doi.org/10.1016/S0024–4937(96)00019–9

Janák M., Mikuš T., Pitoňák P. & Spišiak J. 2009: Eclogites overprinted in the granulite facies from the Ďumbier Crystalline Complex (Low Tatra Mountains, Western Carpathians). *Geologica Carpathica* 60, 193–204.

Janák M., Méres Š. & Medaris G. Jr. 2020: Eclogite facies metaultramafite from the Veporic Unit (Western Carpathians, Slovakia). *Geologica Carpathica*, 71, 209–220. https://doi.org/10.31577/GeolCarp.71.3.1

Janoušek V., Moyen J.–F., Martin H, Erban V. & Farrow C. 2016: Geochemical modelling of igneous processes – Principles and recipes in R language. Bringing the Power of R to a geochemical community. *Springer–Verla*g, Berlin, Heidelberg. https://doi.org/10.1007/978–3–662–46792–3

Johnson T., Yakymchuk C. & Brown M. 2021: Crustal melting and suprasolidus phase equilibria: From first principles to the state-of-the-art. *Earth-Science Reviews* 221, 103778. https://doi.org/10.1016/j.earscirev.2021.103778

Kendrick J. & Yakymchuk C. 2020: Garnet fractionation, progressive melt loss and bulk composition variations in anatectic metabasites: Complications for interpreting the geodynamic significance of TTGs. *Geoscience Frontiers*11, 745–763. https://doi.org/10.1016/j.gsf.2019.12.001

Kohút M. 2020: Geochemistry and provenance of the metasedimentary rocks from the Tatric Unit basement of the Western Carpathians. *Geochémia 2020, Proceedings from Conference*, Bratislava 3.12.2020, 54–59 (in Slovak).

Kohút M. & Larionov A.N. 2021: From subduction to collision: genesis of the Variscan granitic rocks from the Tatric Superunit (Western Carpathians, Slovakia). *Geologica Carpathica* 72, 96–113. https://doi.org/10.31577/GeolCarp.72.2.2

Kohút M. & Nabelek P.I. 2008: Geochemical and isotopic Sr, Nd and O constraints on sources for Variscan granites in the Western Carpathians – implications for crustal structure and tectonics. *Journal of Geosciences* 53, 307–322. https://doi.org/10.3190/jgeosci.033

Kohút M., Kotov A.B., Salnikova E.B. & Kovach V.P. 1999: Sr and Nd isotope geochemistry of Hercynian granitic rocks from the Western Carpathians – implications for granite genesis and crustal evolution. *Geologica Carpathica* 50, 477–487.

Kolb M., Quadt A.V. Peytcheva I., Heinrich C.A., Fowler S.S. & Cvetković V. 2013: Adakite–like and Normal Arc Magmas: Distinct Fractionation Paths in the East Serbian Segment of the Balkan–Carpathian Arc. *Journal of Petrology* 54, 421–451. https://doi.org/10.1093/petrology/egs072

Konečný P., Kusiak M.A. & Dunkley D.J. 2018: Improving U–Th–Pb electron microprobe dating using monazite age references. *Chemical Geology* 484, 22–35. https://doi.org/10.1016/j.chemgeo.2018.02.014

Korikovsky S.P., Janák M. & Lupták B. 1998: Phase relations in olivine–orthopyroxene–chlorite–spinel–hornblende metaultramafics from the Malá Fatra Mts., Western Carpathians. *Geologica Carpathica* 49, 369–376.

Koutek J. 1931: Etudes geologiques dans la partie nord-ouest de la Basse Tatra. *Sborník Ústředního Ústavu Geologického ČSR* IX, 413–613 (in French and Czech).

Kráľ J. 1994: Strontium isotopes in granitic rocks of the Western Carpathians. *Mitteilungen der Österreichischen Geologischen Gesellschaft* 86, 75–81.

Kroner U. & Romer R.L. 2013: Two plates – Many subduction zones: The Variscan orogeny reconsidered. *Gondwana Research* 24, 298–329. https://doi.org/10.12789/geocanj.2014.41.059

Laurent O., Martin H., Moyen J. F. & Doucelance R. 2014: The diversity and evolution of late–Archean granitoids: evidence for the onset of ‚modern–style' plate tectonics between 3.0 and 2.5 Ga. *Lithos* 205, 208–235. https://doi.org/10.1016/j.lithos.2014.06.012

Laurent O., Couzinié S., Zeh A., Vanderhaeghe O., Moyen J.F., Villaros A., Gardien V. & Chelle–Michou C. 2017a: Protracted, coeval crust and mantle melting during Variscan late–orogenic evolution: U–Pb dating in the eastern French Massif Central. *International Journal of Earth Sciences* 106, 421–451. https://doi.org/10.1007/s00531–016–1434–9

Laurent O., Zeh A.,Gerdes A., Villaros A., Gros K. & Słaby E. 2017b: How do granitoid magmas mix with each other? Insights from textures, trace element and Sr–Nd isotopic composition of apatite and titanite from the Matok pluton (South Africa). *Contributions to Mineralogy and Petrology* 172, 1–12. https://doi.org/10.1007/s00410–017–1398–1

Liégeois J.–P., Navez J., Hertogen J. & Black R. 1998: Contrasting origin of post collisional high–K calc–alkaline and shoshonitic versus alkaline and peralkaline granitoids: the use of sliding normalization. *Lithos* 45, 1–28. https://doi.org/10.1016/S0024-4937(98)00023-1

Ludwig K. 2009: SQUID 2: A User's Manual. *Berkeley Geochronology Center Special Publication* 5, 1–110.

Ludwig K.R. 2012: User's Manual for ISOPLOT/Ex 3.75. A Geochronological Toolkit for Microsoft Excel. *Berkeley Geochronology Center Special Publication* 5.

Magna T., Janoušek V., Kohút M., Oberli F. & Wiechert U. 2010: Fingerprinting sources of orogenic plutonic rocks from Variscan belt with lithium isotopes and possible link to subduction-related origin of some A-type granites. *Chemical Geology* 274, 94–107. https://doi.org/10.1016/j.chemgeo.2010.03.020

Majzlan J., Chovan M., Hurai V. & Luptáková J. 2020a: Hydrother-

mal mineralisation of the Tatric Superunit (Western Carpathians, Slovakia): I. A review of mineralogical, thermometry and isotope data. *Geologica Carpathica* 71, 85–112. https://doi.org/10.31577/GeolCarp.71.2.1

Majzlan J., Chovan M., Kiefer S., Gerdes A., Kohút M., Siman P., Konečný P., Števko M., Finger F., Waitzinger M., Biroň A., Luptáková J., Ackerman L. & Hora J.M. 2020b: Hydrothermal mineralisation of the Tatric Superunit (Western Carpathians, Slovakia): II. Geochronology and timing of mineralisations in the Nízke Tatry Mts. *Geologica Carpathica* 71, 113–133. https://doi.org/10.31577/GeolCarp.71.2.2

Maraszewska M., Broska I. & Kurylo S. 2019a: Hybrid I/S nature of Prašivá granite type, Low Tatra pluton: Evidence from mineralogical data. In: Proceedings of Geologica Carpathica 70 Conference. Bratislava, 91–94.

Maraszewska M., Broska I., Kurylo S. & Bezák V. 2019b: Rock-forming and accessory minerals from contrasting granite types of the Dumbier crystalline complex (Nízke Tatry Mts, Western Carpathians). In: *Zborník Petros 2019*, 40.

Miller C.F., Furbish D.J., Walker B.A., Claiborne L.L., Koteas G.C., Bleick H.A. & Miller J.S. 2011: Growth of plutons by incremental emplacement of sheets in crystal–rich host: Evidence from Miocene intrusions of the Colorado River region, Nevada, US. *Tectonophysics* 500, 65–77. https://doi.org/10.1016/j.tecto.2009.07.011

Montel J.–M. 1993:A model for monazite/melt equilibrium and application to the generation of granitic magmas. *Chemical Geology* 110, 127–146. https://doi.org/10.1016/0009–2541(93)90250–M

Moussallam Y., Schneider D.A., Janák M., Thöni M. & Holm D.K. 2012: Heterogeneous extrusion and exhumation of deep-crustal Variscan assembly: geochronology of the Western Tatra Mountains, northern Slovakia. *Lithos* 144–145, 88–108. https://doi.org/10.1016/j.lithos.2012.03.025

Moyen J.-F. 2009: High Sr/Y and La/Yb ratios: the meaning of the "adakitic signature". *Lithos* 112, 556–574. https://doi.org/10.1016/j.lithos.2009.04.001

Moyen J-F., Laurent O., Chelle–Michou C., Couzini´e S., Vanderhaeghe O., Zeh A., Villaros A. & Gardien V. 2017: Collision vs. subduction–related magmatism: two contrasting ways of granite formation and implications for crustal growth. *Lithos* 277, 154–177. https://doi.org/10.1016/j.lithos.2016.09.018

Moyen J.-F., Janoušek V., Laurent O., Bachmann O., Jacob J–B., Farina F., Fiannacca P. & Villaros A 2021: Crustal melting vs. fractionation of basaltic magmas: Part 1, Granites and paradigms. *Lithos*. 402–403. 106291. https://doi.org/10.1016/j.lithos.2021.106291

Matte Ph. 1986: Tectonic and plate tectonics model for the Variscan Belt of Europe. *Tectonophysics* 126, 329–374. https://doi.org/10.1016/0040-1951(86)90237-4

Müntener O., Kelemen P.B. & Grove T.L. 2001: The role of H_2O during crystallization of primitive arc magmas under uppermost mantle conditions and genesis of igneous pyroxenites: an experimental study. *Contributions to Mineralogy and Petrology* 141, 643–658. https://doi.org/10.1007/s004100100266

Oberc-Dziedzic T., Kryza R., Pin C. & Madej S. 2013: Sequential granite emplacement: A structural study of the late Variscan Strzelin intrusion, SW Poland. *International Journal of Earth Science* 102**,** 1289–1304. https://doi.org/10.1007/s00531–013–0863

Ondrejka M., Li X–H., Vojtko R., Putiš M., Uher P.& Sobocký T. 2018: Permian A–type rhyolites of the Muráň Nappe, Inner Western Carpathians, Slovakia: in–situ zircon U–Pb SIMS ages and tectonic setting. *Geologica Carpathica* 69, 187–198. https://doi.org/10.1515/geoca–2018–0011

Ondrejka M., Uher P., Putiš M., Kohút M., Broska I., Larianov A., Bojan A. & Sobocky T. 2021: Permian A–type granites of the Western Carpathians and Transdanubian regions: products of the Pangea supercontinent breakup. *International Journal of Earth Science (Geol. Rundsch.)* 110, 2133–2155. https://doi.org/10.1007/s00531–021–02064–2

Paces J.B. & Miller J.D. 1993: Precise U–Pb Ages of Duluth Complex and Related Mafic Intrusions, Northeastern Minnesota: Geochronological Insights to Physical, Petrogenic, Paleomagnetic and Tectonomagmatic Processes Associated with the 1.1 Ga Midcontinent Rift System. *Journal of Geophysical Research: Solid Earth* 98, 13997–14013. https://doi.org/10.1029/93JB01159

Paterson S.R., Fowler T.K., Schmidt K.L., Yoshinobu A.S., Yuan E.S. & Miller R. 1998: Interpreting magmatic fabric patterns in plutons. *Lithos* 44, 53–82. https://doi.org/10.1016/S0024–4937(98)00022–X

Patiño Douce A.E. 1999: What do experiments tell us about relative contributions of crust and mantle to the origin of granitic magmas? In: Castro A., Fernandez C., Vigneresse J.L. (Eds.): Understanding Granites: Integrating New and Classical Techniques. *Geological Society of London Special Publications* 168, 55–75. https://doi.org/10.1144/GSL.SP.1999:168.01.05

Pearce J.A., Harris N.W. & Tindle A.G. 1984: Trace element discrimination diagrams for the tectonic interpretation of granitic rocks. *Journal of Petrology* 25, 956–983. https://doi.org/10.1093/petrology/25.4.956

Peccerillo A. & Taylor S.R. 1976: Geochemistry of Eocene calc–alkaline volcanic rocks from the Kastamonu area, Northern Turkey. *Contributions to Mineralogy and Petrology* 58, 63–81. https://doi.org/10.1007/BF00384745

Petrík I. 1982: Biotites of the West Carpathian granitoids: a survey. *Geologický Zborník – Geologica Carpathica* 33, 5, 631–633.

Petrík I. 2000: Multiple sources of the West-Carpathian Variscan granitoids, a review of Rb–Sr and Sm–Nd data. *Geologica Carpathica* 51, 145–158.

Petrík I. & Broska I. 1994: Petrology of two granite types from the Tribeč Mountains, Western Carpathians: an example of allanite (+ magnetite) versus monazite dichotomy. *Geological Journal* 29, 59–78. https://doi.org/10.1002/gj.3350290106

Petrík I. & Kohút M. 1997: The evolution of granitoid magmatism during the Hercynian Orogen in the Western Carpathians. In: Grecula P., Hovorka D. & Putiš M. (Eds.): Geological evolution of the Western Carpathians *Mineralia Slovaca – Monograph*, Bratislava, 235–252.

Petrík I. & Konečný P. 2009: Metasomatic replacement of inherited metamorphic monazite in a biotite–garnet granite from the Nízke Tatry Mountains, Western Carpathians, Slovakia: Chemical dating and evidence for disequilibrium melting. *American Mineralogist* 94, 957–974. https://doi.org/10.2138/am.2009.2992

Petrík I., Broska I. & Uher P. 1994: Evolution of the Western Carpathian granite magmatism: age, source rock, geotectonic setting and relation to the Variscan structure. *Geologica Carpathica* 45, 283–291

Plašienka D., Grecula P., Putiš M., Kováč M. & Hovorka D. 1997: Evolution and structure of the Western Carpathians: An overview. In: Grecula P., Hovorka D. & Putiš M. (Eds.): Geological evolution of the Western Carpathians. *Mineralia Slovaca – Monograph*, Bratislava, 1–24.

Poller U., Janák M., Kohút M. & Todt W. 2000: Early Variscan magmatism in the Western Carpathians: U–Pb zircon data from granitoids and orthogneisses of the Tatra Mountains (Slovakia). *International Journal of Earth Sciences* 89, 336–349. https://doi.org/10.1007/s005310000082

Poller U., Kohút M., Gaab A.S. & Todt W. 2005: Pb, Sr and Nd isotope study of two co–existing magmas in the Low Tatra Mts. Mountains, Western Carpathians Slovakia. *Mineralogy and Petrology* 84, 215–231. https://doi.org/10.1007/s00710-005-0080-x

Putiš M., Kotov A.B., Petrík I., Korikovsky S.P., Madarás J., Salnikova E.B., Yakovleva S.Z., Berezhnaya N.G., Plotkina Y.V., Kovach V.P. Lupták B. & Majdán, M. 2003: Early–vs. Late orogenic granitoids relationships in the Variscan basement of the Western Carpathians. *Geologica Carpathica* 54, 163–174.

Putiš M., Sergeev S., Ondrejka M., Larionov A., Siman P., Spišiak J.,

Uher P. & Paderin I. 2008: Cambrian–Ordovician metaigneous rocks associated with Cadomian fragments in the West-Carpathian basement dated by SHRIMP on zircons: a record from the Gondwana active margin setting. *Geologica Carpathica* 59, 3–18.

Putiš M., Ivan P., Kohút M., Spišiak J., Siman P., Radvanec M., Uher P., Sergeev S., Larionov A., Méres Š., Demko R. & Ondrejka M. 2009: Meta-igneous rocks of the West-Carpathian basement, Slovakia: indicators of Early Paleozoic extension and shortening events. *Bulletin de la Société géologique de France* 180, 461–471. https://doi.org/10.2113/gssgfbull.180.6.461

Rapp R.P. & Watson E.B. 1995: Dehydration melting of metabasalt at 8–32 kbar: implications for continental growth and crust–mantle recycling. *Journal of Petrology* 36, 891–931. https://doi.org/10.1093/petrology/36.4.891

Roddick J.C. & van Breemen O. 1994: U–Pb zircon dating: a comparision of ion microprobe and single grain conventional analysis. In: Radiogenic age and isotopic studies: report 8. *Current Research, Geological Survay of Canada*, 1–9. https://doi.org/10.4095/195164

Rodríguez N., Díaz-Alvarado J., Fernández C., Fuentes P., Breitkreuz C. & Tassinari C.C.G. 2019: The significance of U–Pb zircon ages in zoned plutons: the case of the Flamenco pluton, Coastal Range batholith, northern Chile. *Geoscience Frontiers* 10, 1073–1099. https://doi.org/10.1016/j.gsf.2018.06.003

Sawyer E.W. 1999: Criteria for recognition of partial melting. *Physics and Chemistry of the Earth, Part A: Solid Earth and Geodesy* 24, 269–279. https://doi.org/10.1016/S1464-1895(99)00029-0

Schaltegger U., Fanning C.M., Günther D., Maurin J.C., Schulmann K. & Gebauer D. 1999: Growth, annealing and recrystallization of zircon and preservation of monazite in high-grade metamorphism: conventional and in-situ U–Pb isotope, cathodoluminescence and microchemical evidence. *Contributions to Mineralogy and Petrology* 134, 186–201. https://doi.org/10.1007/s004100050478

Schulmann K., Catalán J. R. M., Lardeaux J. M., Janoušek V. & Oggiano G. 2014: The Variscan orogeny: extent, timescale and the formation of the European crust. *Geological Society of London Special Publications* 405, 1–6. https://doi.org/10.1144/SP405.15

Siegl K. 1970: Fabric anisotropy of Ďumbier granodiorite. *Geologický Zborník – Geologica Carpathica* 21, 327–334.

Skjerlie K.P. & Patiño Douce A.E. 2002: The fluid–absent partial melting of a zoisite–bearing quartz eclogite from 1.0 to 3.2 GPa; implications for melting in thickened continental crust and for subduction–zone processes. *Journal of Petrology* 43, 291–314. https://doi.org/10.1093/petrology/43.2.291

Słaby E., Galbarczyk-Gasiorowska L., Seltmann R. & Müller A. 2007: Alkali feldspar megacryst growth: Geochemical modelling. *Mineralogy and Petrology* 89, 1–29. https://doi.org/10.1007/s00710–006–0135–7

Spišiak J., Mikuš T., Chew D., Vetráková L., Siman P. & Ferenc Š. 2017: Dioritické horniny z Železného (Nízke Tatry): petrológia a geochémia. In: *Zbornik Petros 2017*, 29–62.

Spišiak J., Vetráková L., Chew D., Ferenc Š., Mikuš T., Šimonová V. & Bačík P. 2018: Petrology and dating of the Permian lamprophyres from the Malá Fatra Mts. (Western Carpathians, Slovakia). *Geologica Carpathica* 69, 453–466. https://doi.org/10.1515/geoca-2018-0026

Spišiak J., Vetráková L., Chew D., Ferenc Š., Mikuš T., Šimonová V., Butek J.& Mikuš T. 2021: Permian lamrophyres from the Western Carpathians: a review. *Geological Society London Special Publications* 513, 297–321. https://doi.org/10.1144/SP513-2020-237

Stacey J. & Kramers J. 1975: Approximation of terrestrial lead isotope evolution by a two–stage model. *Earth Planetary Science Letters* 26, 207–221.

Sylvester P.J. 1998: Post-collisional strongly peraluminous granites. *Lithos* 45, 29–44. https://doi.org/10.1016/S0024–4937(98)00024–3

Tarney J. & Jones C.E. 1994: Trace element geochemistry of orogenic igneous rocks and crustal growth models. *Journal of the Geological Society* 151, 855–868. https://doi.org/10.1144/gsjgs.151.5.0855

Uher P., Kohút M. & Putiš M. 2011: Hercynian dioritic rocks of the Western Carpathians: tracers of crustal – mantle interactions. *Travaux géophysique* 40, 86.

Vavra G., Gebauer D., Schmid R. & Compston W. 1996: Multiple zircon growth and recrystallization during polyphase Late Carboniferous to Triassic metamorphism in granulites of the Ivrea Zone (Southern Alps): an ion microprobe (SHRIMP) study. *Contributions to Mineralogy and Petrology* 122, 337–358. https://doi.org/10.1007/s004100050132

Vernon R., Johnson S. & Melis E. 2004: Emplacement–related microstructures in the margin of a deformed pluton: The San Jose tonalite, Baja California, Mexico. *Journal of Structural Geology* 26, 1867–1884. https://doi.org/10.1016/0012-821X(75)90088-6

Villaseca C., Barbero L.& Hereros V. 1998: A reexamination of the typology of peraluminous granite types in intracontinental orogenic belts. *Transactions of the Royal Society of Edinburgh: Earth Sciences* 89, 113–119. https://doi.org/10.1017/S0263593300007045

Villaseñor G., Catlos E.J., Broska I., Kohút M., Hraško Ľ., Aguilera K., Etzel T., Kyle J.R. & Stockli D.F. 2021: Evidence for widespread mid–Permian magmatic activity related to rifting following the Variscan orogeny (Western Carpathians). *Lithos* 390–391, 106083. https://doi.org/10.1016/j.lithos.2021.106083

Watkins J.M., Clemens J.D. & Treloar P.J.2007: Archaean TTGs as sources of younger granitic magmas: melting of sodic metatonalites at 0.6 to 1.2 GPa. *Contributions toMineralogy and Petrology* 154, 91–110. https://doi.org/10.1007/s00410-007-0181-0

Weinberg R.F.& Hasalová P. 2015: Water–fluxed melting of the continental crust: a review. *Lithos* 212–215, 158–188. https://doi.org/10.1016/j.lithos.2014.08.021

Williams I.S. 1998: U–Th–Pb geochronology by ion microprobe. *Reviews in Economic Geology* 7, 1–35. https://doi.org/10.5382/Rev.07.01

Xu W., Zhang H., Luo B., Guo L. & Yang H. 2015: Adakite–like geochemical signature produced by amphibole–dominated fractionation of arc magmas: An example from the Late Cretaceous magmatism in Gangdese belt, south Tibet. *Lithos* 232, 197–210. https://doi.org/10.1016/j.lithos.2015.07.001

Zen E. 1986: Aluminium enrichment in silicate melts by fractional crystallization: some mineralogic and petrographic constraints. *Journal of Petrology* 27, 1095–1117. https://doi.org/10.1093/petrology/27.5.1095

Zhao Z.F., Dai L.Q. & Zheng Y.F. 2013: Postcollisional mafic igneous rocks record crust–mantle interaction during continental deep subduction. *Scientific Reports* 3, 3413. https://doi.org/10.1038/srep03413

Electronic supplementary material is available online:

SM1 "Whole rock and trace element geochemistry of investigated granitoid types with localities and description" at http://geologicacarpathica.com/data/files/supplements/GC-73-4-Maraszewska_SM1.xlsx

SM2 "Zircon U–Th–Pb isotopes analysed by SHRIMP-SIMS for Low Tatra Mts. Granitoids" at http://geologicacarpathica.com/data/files/supplements/GC-73-4-Maraszewska_SM2.xlsx

SM3 "Whole dataset of results of monazite U–Th-total Pb dating in Low Tatra Mts. Granitoids" at http://geologicacarpathica.com/data/files/supplements/GC-73-4-Maraszewska_SM3.xlsx